GEOLOGICAL SURVEY OF CANADA

DEPARTMENT OF ENERGY, MINES AND RESOURCES, OTTAWA

PAPER 74-59

MAGNETIC PROPERTIES OF PYRRHOTITE AND THEIR USE IN APPLIED GEOLOGY AND GEOPHYSICS

E.J. SCHWARZ

1975

Energy, Mines and Resources Canada
Énergie, Mines et Ressources Canada

GEOLOGICAL SURVEY
PAPER 74-59

MAGNETIC PROPERTIES OF PYRRHOTITE AND THEIR USE IN APPLIED GEOLOGY AND GEOPHYSICS

E.J. SCHWARZ

Available by mail from *Information Canada*, Ottawa, K1A 0S9

from the Geological Survey of Canada
601 Booth St., Ottawa, K1A 0E8

and

Information Canada bookshops in

HALIFAX — 1683 Barrington Street
MONTREAL — 640 St. Catherine Street W.
OTTAWA — 171 Slater Street
TORONTO — 221 Yonge Street
WINNIPEG — 393 Portage Avenue
VANCOUVER — 800 Granville Street

or through your bookseller

A deposit copy of this publication is also available
for reference in public libraries across Canada

Price - Canada: $2.50
Other Countries: $3.00

Catalogue No. M44-74-59

Price subject to change without notice

Information Canada
Ottawa
1975

Contents

Illustrations

Contents (cont'd)

MAGNETIC PROPERTIES OF PYRRHOTITE AND THEIR USE IN APPLIED GEOLOGY AND GEOPHYSICS

ABSTRACT

This paper presents an overview of magnetic properties of pyrrhotite ($Fe_{1-x}S$, $0 \leq x \leq 0.13$) *of interest in geological and geophysical applications. The first part shows the strong dependence of the relevant magnetic properties on the chemical composition, and cation vacancy ordering, and standards are set up for the analysis of natural pyrrhotites. The thermomagnetic method of analysis for composition is discussed in comparison with other existing methods. In the second part a number of practical applications are discussed including the spatial distribution of pyrrhotite types, both in massive sulphide deposits and in relation to types of wall-rocks, remanent magnetization, fabric, and type of concomitant magnetic anomaly expected. The third part presents a theoretical consideration of the dependence of the free energy on vacancy ordering. Calculation of the average atomic magnetic moment in* Fe_7S_8 *suggests that considerable non-ionic bonding takes place in the structure.*

RÈSUMÈ

L'auteur expose les propriétés magnétiques de la pyrrhotine ($Fe_{1-x}S$, $0 \leq x \leq 0.13$) *lesquelles peuvent être appliquées en géologie et en géophysique. La première partie de l'exposé démontre que les propriétés magnétiques en question dépendent particulièrement de la composition chimique et de l'agencement des lacunes (cations manquants), et détermine les règles de l'analyse des pyrrhotines naturelles. La méthode thermomagnétique d'analyse élémentaire y est comparée à d'autres méthodes connues. Dans la deuxième partie, l'auteur traite d'un certain nombre d'applications pratiques, telles que l'étude de la répartition des divers types de pyrrhotites qu'on rencontre dans les gîsements de sulfures massifs ou en association avec divers types de roches encaissantes, de l'aimantation remanente, de la texture, et l'étude du type d'anomalie magnétique concomitante qu'on peut en attendre. La troisième partie considère, du point de vue théorique, la relation existant entre l'énergie libre et l'agencement des lacunes. Selon les calculs du moment magnétique atomique moyen dans le cas de* Fe_7S_8, *on est amené à penser que les liaisons non-ioniques jouent un rôle considérable dans la structure de ce minéral.*

INTRODUCTION

Pyrrhotite is used here as a collective term for the hexagonal and pseudohexagonal iron sulphides of composition $Fe_{1-x}S$. In general, pyrrhotite is found in metal sulphide (ore) deposits in strong concentrations and/or is finely dispersed. However, its occurrence is more wide-spread in some basic intrusives, in some metamorphic formations and in some ocean floor basalts and marine sediments. It has been frequently observed in lunar rocks.

There are only a few magnetic minerals. With the exception of pyrrhotite, they are essentially oxides of iron in which some of the iron may have been replaced by other elements notably titanium. Much is known of the magnetic properties of these oxides, in particular of those (Fe_3O_4, γFe_2O_3) which possess a spinel structure, because of the interest in synthetic ferrites for various technical applications. In contrast, pyrrhotite has attracted little interest from physicists. However, the strongly anisotropic ferrimagnetism displayed by some of these iron sulphides, the high electrical conductivity, and the occurrence in sulphide ore deposits make pyrrhotite a mineral of extreme interest in mining geophysics. Furthermore, from a geological point of view, the phase relations between various pyrrhotite types and sulphides of economic interest in sulphide deposits are important in elucidating the genesis of these deposits. The study of fabric in sulphide deposits and their wall-rocks would prove useful in unravelling the tectonic history of these deposits. Finally, the ferrimagnetism and the occurrence of the mineral in other rock types may attract the attention of people interested in the interpretation of magnetic anomalies and in paleomagnetism. It appeared worthwhile, therefore, to investigate systematically the magnetic properties of pyrrhotite with such applications in mind.

Ward (1970) reviewed the mineralogical aspects and the phase relations of pyrrhotites. Although some magnetic properties as well as Mössbauer results are discussed in that review, a much more detailed reconsideration of the present knowledge of the magnetic properties is desirable. The basis for this reconsideration is the detailed magnetic phase diagrams which recently have been obtained by Schwarz and Vaughan (1972). Earlier attempts to arrive at magnetic phase diagrams are due to Haraldsen (1941 a, b).

Finally, the effect of vacancy order and magnetic order in the crystal lattice is of theoretical interest. The mode of change of the magnetic susceptibility with temperature depends strongly on the chemical composition, and for compositions around Fe_9S_{10}, on the thermal history. The latter is generally regarded to be caused by order-disorder transitions of the vacant cation sites on the basis of Néel's (1948, 1953) theory of ferrimagnetism (Hirone *et al.*, 1954; Lotgering, 1956). Lotgering has considered these transitions on the basis of the

Original manuscript submitted: May 28, 1974.
Approved for publication: September 23, 1974.

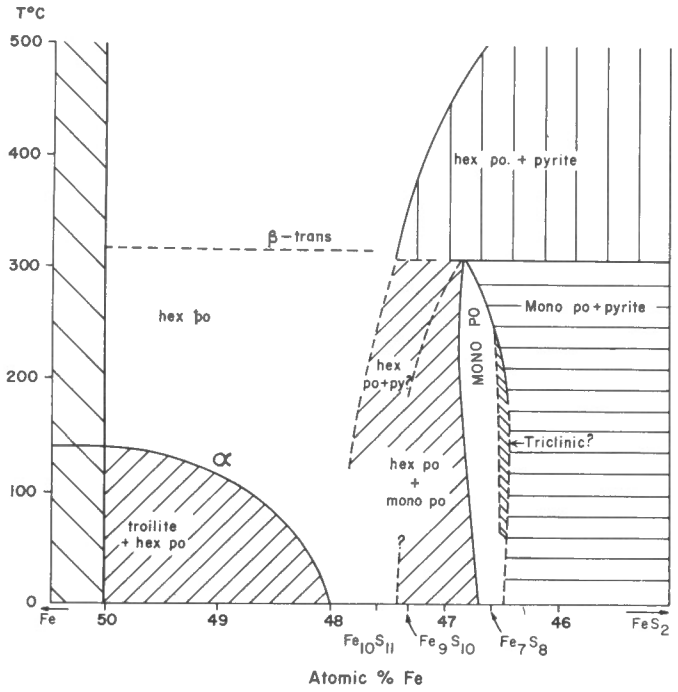

Figure 1

Phase diagram of the pyrrhotite group. Po and py represent pyrrhotite and pyrite respectively and hex and mono indicate hexagonal and monoclinic crystal symmetry.

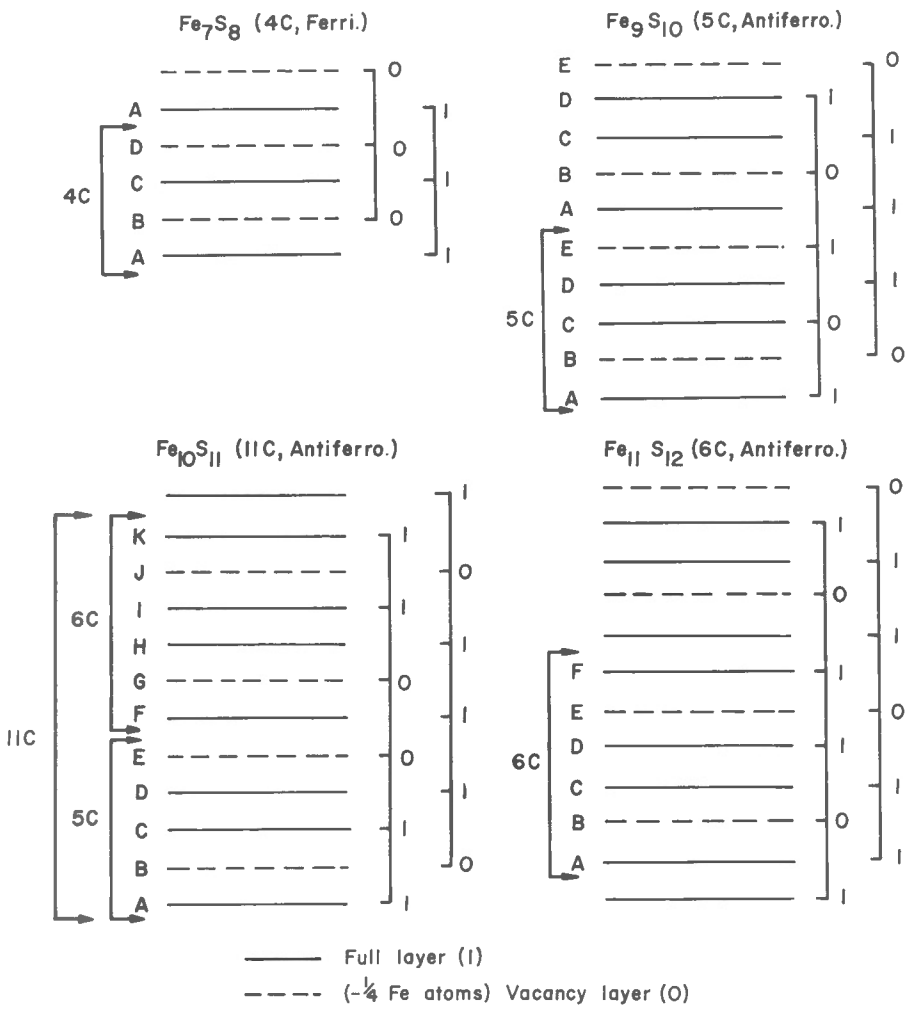

Figure 2

Schematic representation of the proposed structure of some pyrrhotite compositions. Ferri and antiferro represent ferrimagnetic and antiferromagnetic structures.

Bragg-Williams (1935) theory in a very simplified manner assuming that antiferromagnetism is compatible with an even and random distribution of the vacancies over both interpenetrating sublattices which oppose each other magnetically. However, it can be argued that this is not a satisfactory assumption as it involves ordering during heating and would lead to a decrease in crystal symmetry hitherto not observed at the transition temperature T_γ or "anti-Curie point". Furthermore, as Mössbauer results (Ward, 1970; Vaughan and Ridout, 1970) show the absence of a preferred location of Fe^{3+}, these theoretical considerations can be extended to arrive at a more detailed result using antiferromagnetic vacancy-ordered models proposed by Schwarz and Vaughan (1972) for the intermediate compositions.

Acknowledgments

Samples of natural pyrrhotite were obtained from various mines operated by Falconbridge Nickel Mines Ltd., The International Nickel Company of Canada Ltd., and Noranda Mining and Smelting Ltd. I thank the geological staff of these Companies for their cooperation. A portion of Part III of this paper was prepared during a visit to the Geophysical Institute of the University of Tokyo. Dr. C.M. Carmichael of the University of Western Ontario kindly read the manuscript and his comments were very helpful in improving the readability of this paper.

PART I

BASIC DATA

Many magnetic minerals exhibit ionic or pseudo-ionic bonding due to electrostatic interactions between the cations and anions. The cations take up sites between the larger anions such as O^{2-} which usually show dense packing. The magnetic exchange forces between the paramagnetic cations fall off exponentially with distance so that in these minerals an exchange mechanism is required which makes use of an anion close to a pair of cations. This type of exchange has been called superexchange (Anderson, 1950). The strength of the magnetic interaction depends on the degree of "overlap" of 3d electron orbits of the cations with the stretched orbits of 2p electrons of O^{2-} or 3p electrons of S^{2-}. Thus, the angles formed by cation-anion-cation clusters play an important role in the interaction (Wollan, 1960) establishing a basic relation between crystal structure and magnetism. However, the indications are that a very considerable part of the bonding in $Fe_{1-x}S$ is due to the occurrence of collective electron orbits giving rise to groups like $(S_n)^{2-}$ where $n\geq$ (integer).

In pyrrhotite $Fe_{1-x}S$, where $0\leq x \lesssim 0.13$, two distinct crystallographic transitions occur which have been labelled α and β by Haraldsen (1941a, b) as shown on Figure 1. The transition temperature, which is about 140°C for FeS (x=0) decreases rapidly with Fe deficiency ($x\neq 0$). The β transition seems to occur at 320°C across the compositional field. Both transitions appear to coincide with abrupt changes in the magnetic susceptibility as shown by Figure 1. The change in susceptibility at or near the α transition temperature (T_α) is strong and is thought to be related to the rotation of the cation spin magnetic moments from parallel to the C axis to the basal plane (Andresen and Torbo, 1967). Above T_β, all compositions are hexagonal (e.g. Taylor, 1970). This constitutes an increase in symmetry for the Fe deficient composition Fe_7S_8 (x=0.125) which suggests the disappearance at T_β of a vacancy ordered superstructure of low symmetry.

In the temperature-composition field between the α (or 20°C) and β transitions various superstructures have been reported in particular for synthetic samples. However, a number of structures such as 2A, 4C; 2A, 5C; 2A, 6C; 2A, 11C are now rather well established (e.g. Morimoto *et al.*, 1970) and they can be understood on the basis of different stacking orders of elements of Bertaut's (1953) cell for Fe_7S_8 (Vaughan *et al.*, 1971; Schwarz and Vaughan, 1972). On the other hand, the very strong change in susceptibility - Haraldsen's (1941a) γ transition - observed for vacancy concents of about 10%, has not been clearly associated with a crystallographic transition. This change shows thermal hysteresis and has been ascribed to a vacancy (and Fe^{3+}) disorder-order transition (Lotgering, 1956) or to a change in the ordering pattern of the vacancies (Hirone *et al.*, 1954; Schwarz and Vaughan, 1972). The only pertinent information available is Haraldsen's (op. cit) observation that at T_γ, the change of the susceptibility is accompanied by an abrupt change in the axial ratio c/a. The thermal change of the susceptibility does not yield evidence for any other structural changes than the α, β, and γ transitions.

Magnetic Structure

The chemical composition of pyrrhotite can be represented by $Fe_{1-x}S$ where $0\leq x <0.13$. However, not all values of x appear to occur in natural pyrrhotite as only rational Fe/S ratios are observed (Moriomoto *et al.*, 1970; Vaughan *et al.*, 1971).

Only for the composition FeS (x=0), are all octahedral cation sites in the crystal lattice occupied. These sites are arranged in layers perpendicular to the crystallographic C axis. Below the Curie temperature, the magnetic moments of the cations within each basal plane ($\perp$C axis) tend to be parallel, and to be antiparallel to the moments of the cations on the planes directly below and above. Thus, the magnetic structure can be represented by two magnetic sublattices each consisting of layers with parallel (strictly at T=0°K) cation magnetic moments. Both sublattices oppose each other magnetically, and are equal either for x=0 or for random vacancies ($x\neq 0$). This is called an antiferromagnetic structure, and the rotation of the total sublattice magnetizations under the action of a magnetic field produces a small positive magnetic susceptibility. A special form of antiferromagnetism is caused by the natural cancellation of non-zero magnetic moments of unit cells stacked along the C-axis. On the other hand, a concentration of vacant sites (which do not contribute to the total magnetization) on one sublattice generates a difference in the sublattice magnetizations and an appreciable susceptibility. This type of structure is called ferrimagnetism. Information on the magnetic structure can be obtained by magnetizing a material to saturation and by heating experiments.

Models to account for the crystallographic and magnetic properties of various compositions $Fe_{1-x}S$ were proposed by Schwarz and Vaughan (1972), and are also shown on Figure 2. The model for Fe_7S_8 consists of an alternation of filled and vacancy containing layers as proposed by Bertaut (1953). The models for the other compositions are built up by using different stacking orders of filled and vacancy containing layers to account for (1) chemical composition, (2) crystal structure, and (3) magnetic structure as shown on Figure 2. These models are discussed in detail by Schwarz and Vaughan (1972).

The diagnostic value of magnetic parameters

Two intrinsic magnetic properties are of high diagnostic value: the Curie temperature and the saturation magnetization. The Curie temperature depends rather strongly on the Fe/S ratio so that precise determinations of this ratio can be made from the thermomagnetic curve which represents the change in magnetization with temperature. The Curie temperature represents the temperature at which long-range magnetic order due to magnetic interactions between the cations disappears during heating and reappears during subsequent cooling. On the other hand, the saturation magnetization, which is the maximum magnetization a material can acquire in an applied magnetic field, poses a problem in the case of polycrystalline pyrrhotite. The problem is that the saturation magnetization cannot be measured unless one has either a perfect crystal of sufficient size or is in the position to use a constant applied field of at least 20,000 oe. Besnus and Meyer (1964) have measured saturation moments of up to 22.5 c.g.s. electromagnetic units (emu/g) at 20°C for a natural pyrrhotite of which no particulars were given. The difficulty of magnetizing unoriented crystals of pyrrhotite, as often encountered in nature, to saturation is due to the extremely strong magnetocrystalline anisotropy. This prevents the alignment of the cation magnetic moments parallel to the C axis in fields normally attainable. Consequently, the saturation moment must be estimated from the magnetization curve assuming random orientation of the crystals and truly uniaxial anisotropy. This procedure usually yields saturation moments up to approximately 24 emu/g. In general, these estimates will be too high in a sample consisting of small crystals which can move independently of each other. In natural pyrrhotite, the saturation magnetization is useful in estimating the abundance of the magnetic phases before heating as discussed in a later section.

A third magnetic parameter, the anisotropy of magnetic susceptibility, is used in the present study. In general, magnetic anisotropy is caused almost entirely by two factors (1) the intrinsic magnetocrystalline anisotropy and (2) a non-intrinsic component due to the non-spherical shape of natural grains. The magnetocrystalline anisotropy greatly predominates in ferrimagnetic pyrrhotite. Consequently, anisotropy in rocks containing even a small fraction (e.g. 10% or more) of pyrrhotite is diagnostic for a preferred orientation of the crystals. The latter may arise from tectonic stresses. Exsolution lamellae not parallel to the basal plane which holds the direction of maximum susceptibility, may cause a decrease in the anisotropy. However, Graterol and Naldrett (1971) state that pentlandite, which frequently is observed in Sudbury ore, occurs as oriented flames along the basal parting in pyrrhotite. This would have a very small effect on the anisotropy due to crystal orientation.

Techniques to distinguish between coexisting pyrrhotite types

It is well known that many pyrrhotite samples obtained from natural deposits are not homogeneous but consist of a least two coexisting phases. To make a distinction between these phases is highly relevant to many studies such as partition of Ni and Co (Vaughan *et al.*, 1971). There are several techniques to arrive at a qualitative or quantitative distinction.

1. Etching (e.g. Arnold, 1967; Schwarz, 1968) by chromic acid or a solution of, for instance, HI. A contrast in magnetic properties of the phases in polished sections can be made visible by using a demagnetized magnetite colloid after magnetizing the polished section and observation with a microscope (Schwarz, 1968; Schwarz and Harris, 1970). The proportions of etched/unetched or non-magnetic/magnetic pyrrhotite can be estimated (Fig. 3).

2. The use of an electron microprobe may allow the determination of the composition of the phases and an estimate of the relative abundance (Schwarz and Harris, 1970). However, the prerequisites are accurate standards and, in particular, rather coarse (≥1μm) intergrowths of the phases. Even in natural samples, the latter condition is often not fulfilled (Arnold, 1967).

3. Magnetic separation after grinding (Hayase *et al.*, 1963) has the advantage of physically separating the phases to some degree. The separated fractions must be subsequently subjected to X-ray or magnetic techniques to obtain their composition, or structure and the ratio of the weights of the fractions (magnetic and non-magnetic) will yield a rough estimate of the relative abundance. A variant of this method suggested by Ward (1970) requires both separation and heating and is recommended if physical separation is required and if the sample consists of a ferrimagnetic phase, a phase which shows the antiferromagnetic-ferrimagnetic transition, and a consistently antiferromagnetic phase between 20 and 320°C. A three-phase mixture has not yet been reported to occur in nature.

4. The X-ray diffraction method of analysis is based on the (102) spacing (Desborough and Carpenter, 1965; Arnold, 1967; Graham, 1969; Sugaki and Shima, 1966). This method is the most widely used and allows a quantitative determination of the compositions and relative abundance of coexisting phases. However, the interpretation of the powder diffraction patterns hinges on the distinction of the hexagonal peak and both monoclinic peaks. The difficulty is that the hexagonal peak and one of the monoclinic peaks show considerable overlap. The distinction depends entirely on the assumption that both monoclinic peaks are of the same intensity regardless of the complex variety of superstructures in the central portion of the pyrrhotite field below 320°C some of which may in fact be orthorhombic according to Morimoto *et al.*, (1970). Furthermore, there appears to be a chance to bias the results by grinding.

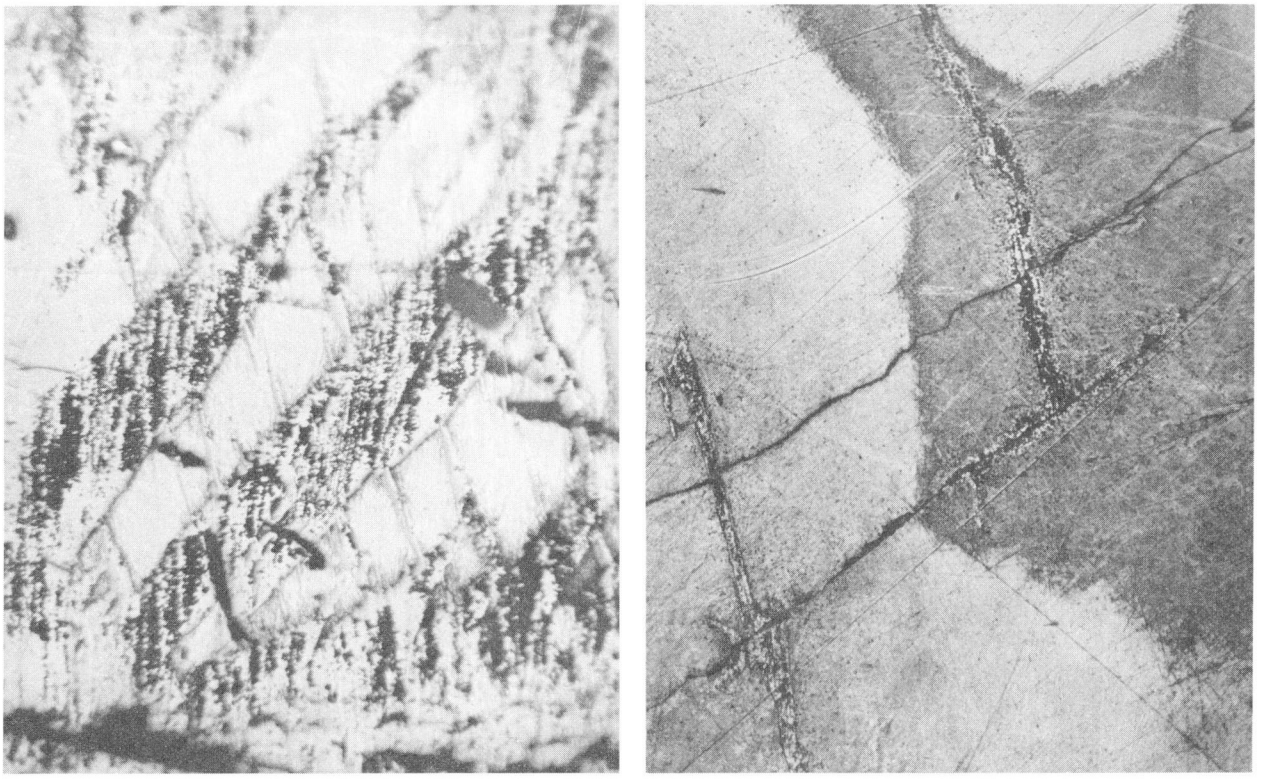

Figure 3. Etched polished surfaces treated with magnetite colloid showing co-existence of a magnetic (Fe_7S_8) and a non-magnetic (Fe_9S_{10}) pyrrhotite type.

5. The thermomagnetic method of analysis (Schwarz, 1968; Schwarz and Harris, 1970; Schwarz, 1973) is based on splitting up anomalous thermomagnetic curves into parts that can each be ascribed to one phase. The Curie temperature of each part yields the composition of one phase. The magnetization at 20° before heating is a reliable measure of the abundance of the ferrimagnetic phase. No magnetic separation is needed, the interpretation of the experimental results is simple and straightforward, and the method is generally applicable whatever the size of the intergrowths. The method requires heating of the specimens up to 310°C and must therefore not be applied to powdered samples unless precautions are taken to prevent loss of sulphur and oxidation. Thermomagnetic curves, which show a normal decrease of the magnetization during heating resulting in single, well-defined transition temperatures, are produced by single-phase pyrrhotite. The resolution is approximately 1% for the antiferromagnetic phase and 0.1% for the ferrimagnetic phase if virtually pure pyrrhotite samples are used.

Magnetic properties of synthetic pyrrhotites

In the present context, synthetic pyrrhotites are of importance as their magnetic properties provide standards in the investigation of natural pyrrhotites. The advantage of using synthetic materials for this purpose is of course that composition can be closely controlled. However, care must be taken in the application of magnetic standards obtained for pure $Fe_{1-x}S$ as the addition of, for instance, 1% by weight of Ni appears to noticeably lower the Curie temperature (Vaughan *et al.*, 1971), and such Ni concentrations have been observed in Fe_9S_{10}.

There are several ways to synthesize $Fe_{1-x}S$ (e.g. Lotgering, 1956; Sugaki and Shima, 1966; Andresen and Torbo, 1967) but extreme care must be taken to avoid the introduction of free or bound oxygen as this will produce strongly magnetic Fe_3O_4 at temperatures above 580°C. The method followed in the present case has been discussed in detail by Schwarz and Vaughan (1972). The synthesized samples were sealed in small evacuated silica containers. The field dependence of their magnetization and the dependence of the magnetization in constant fields of 5350 oe were determined with a recording thermomagnetic balance. Due to the high magnetocrystalline anisotropy of pyrrhotite, the saturation magnetization of the ferrimagnetic specimens could not be measured. Instead, the saturation magnetization was estimated from the magnetization curves on the basis of random orientation of the crystals in the sample and uniaxial magnetic anisotropy. An approximate correction for the diamagnetic contribution of the comparatively heavy containers was applied on the basis of the response of an empty standard container.

Figure 4 shows some typical thermomagnetic curves for synthetic samples of different composition. These have been discussed in detail by Schwarz and Vaughan (1972) but they will be summarized here as they form an essential part in the discussion of more practical results which are emphasized in the present paper. The α, β, and γ transitions are easily recognized as well as a reversible, magnetic transition at the Curie temperature T_c. The temperatures of annealing (T_A) of the samples prior to the measurements are also indicated. The curve for FeS (Fig. 4A) suggests an antiferromagnetic structure complicated by the α transition and paramagnetism prevailing above T_β. The curve for Fe_7S_8 (Fig. 4B)

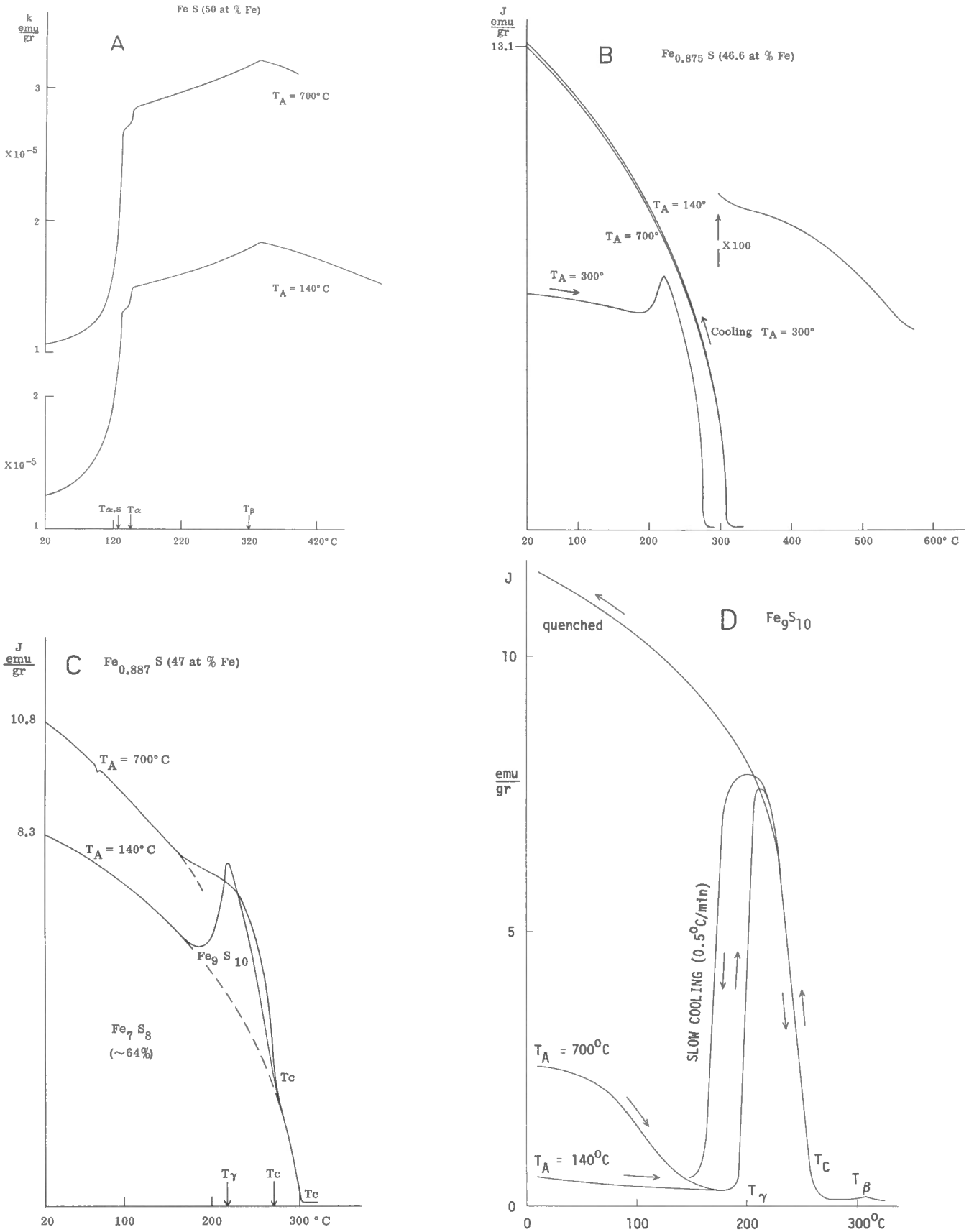

Figure 4. Thermomagnetic curves showing the strong dependence of the magnetization (J) on the temperature and on the chemical composition.

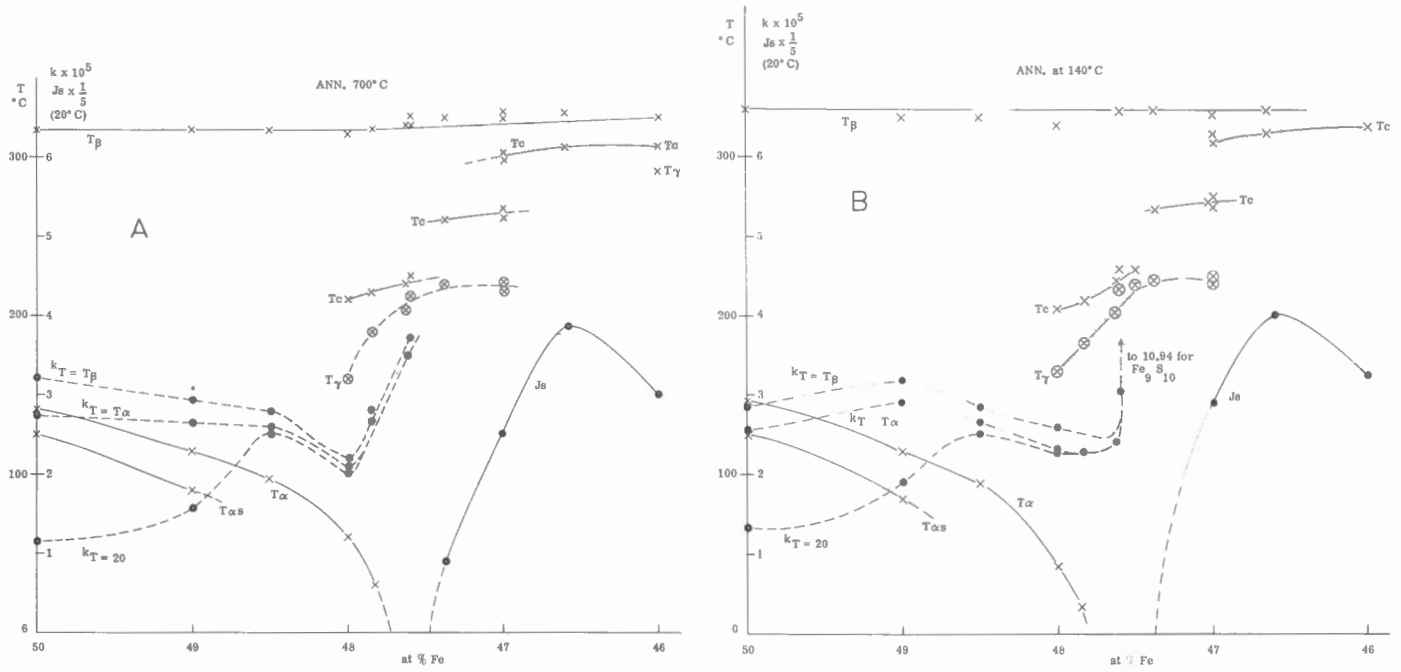

Figure 5. Magnetic phase diagram obtained by compilation of the thermomagnetic results for individual compositions annealed at 140°C for 2½ months (A) and at 700°C for 14 days (B). J and k indicate the estimated saturation magnetization and magnetic susceptibility; the latter at the temperatures 20°C, T_α, and T_β.

shows a normal change of the magnetization (J) with temperature (T) and a single Curie temperature at 310°C*. The intensity of magnetization (J) acquired in a strong magnetic field (H) at 20°C (13.1 emu/g) may be used as a standard in determining the Fe_7S_8 content as discussed below. On the other hand, an abnormal mode of change of the magnetization is noted for the sample of bulk composition $Fe_{0.887}$ (Fig. 4C). Following the method described earlier (Schwarz, 1968) which was tested with an electron microprobe on a suitable sample (Schwarz and Harris, 1970), this curve is split into two parts each showing a Curie point. One of these parts represents a normal change of J (T) with T_c = 310°C which suggests Fe_7S_8. The magnetization before heating (due essentially only to Fe_7S_8) amounts to 8.3 emu/g. Therefore, the abundance of Fe_7S_8 comes to 8.3/13.1= 64% (wt). The other part is more complicated and shows thermal hysteresis below Tγ but not above Tγ thus suggesting a Curie temperature of 265°C as was also observed for Fe_9S_{10} (Fig. 4D). In this manner, the sample of bulk composition $Fe_{0.887}S$ is shown to consist, in fact, of 64% Fe_7S_8 and 36% Fe_9S_{10}. The use of this technique to obtain the relative abundance of these phases after the 700°C anneal may lead to large errors as equilibration was done well above Tγ (ferrimagnetic-antiferromagnetic transition point) and quenching was only partially effective (complicated X-ray results) so that the Fe_9S_{10} component is ferrimagnetic at 20°C. The technique meets no difficulty of this type if applied to natural pyrrhotites as these were equilibrated at temperatures well below Tγ≈200°C (antiferromagnetic range).

The results of the thermomagnetic measurements are represented in the form of a magnetic phase diagram (*see* also Schwarz and Vaughan, 1972) for each of the temperatures of annealing, and they are shown on Figures 5A and B. The following observations can be made from these diagrams:

1. The susceptibility for $T>T_\alpha$ decreases approximately linearly with a decrease in Fe content in the range between 50 and 48 atomic per cent (at %). More Fe deficient compositions show a strong increase in susceptibility which can only be accounted for by the appearance of imbalance between the sublattices due to vacancy ordering.

2. The magnetic properties are most strongly dependant on the thermal history (annealing) for compositions around Fe_9S_{10} (47.3 at % Fe).

3. The distribution of Curie temperatures does not suggest a continuous change with composition. The data rather indicate a stepwise change suggesting that the Fe/S ratios do not change continuously but that only discrete compositions coexist. These compositions appear to centre around rational Fe/S ratios such as Fe_7S_8 and Fe_9S_{10} where only single Curie temperatures are observed. In that case, two-phase fields can be expected for compositions in the range $1 < Fe/S \leq 0.9$ in addition to the well established two-phase field between Fe_9S_{10} and

*With the exception of the results obtained after the 300°C anneal for 2 months. The Curie point shown by these results corresponds to Fe_9S_{10}. Thus, Fe_7S_8 is not stable at temperatures around 300°C, but is transformed into Fe_9S_{10} and FeS_2.

Fe_7S_8. The present data do not provide enough resolution to check this possibility because the difference in composition between sucessive rational Fe/S ratios becomes smaller with decreasing vacancy content, and T_γ and T_α show a stronger dependency on the composition than T_c in the central portion of the diagrams. Not all rational Fe/S ratios appear to occur as stable phases.

4. Fe_7S_8 (46.6 at % Fe) is the most strongly ferrimagnetic composition and shows normal temperature dependency of its high field magnetization. Thus, the γ transition is not observed. However, the γ transition can occur in samples of bulk composition Fe_7S_8 (Fig. 4) after annealing at 300°C. The Curie temperature is suppressed and corresponds to that of Fe_9S_{10}. Consequently, the explanation is that Fe_9S_{10} was formed and pyrite (Fe S_2) exsolved. This is in agreement with results obtained from other studies (Fig. 1).

5. The thermomagnetic characteristics for samples of higher cation vacancy content than 12.5% (Fe_7S_8) are clearly different from those for samples containing 10% cation vacancies (Fe_9S_{10}) so that a distinction between both pyrrhotites can be made. Here again, the records for the composition $Fe_{0.852}S$ suggest the formation of Fe_9S_{10} (+FeS_2) during the annealing at 300°C.

6. The results for FeS show that the reversible transition antiferromagnetism-paramagnetism occurs at 320°C which corresponds to T_β. This suggest that T_β is the Néel temperature (just as the Curie temperature indicating complete loss of long-range magnetic coupling in the lattice but in antiferromagnetic materials). However, long-range magnetic order disappears at T_c for the strongly Fe deficient compositions where $T_\gamma < T_c < T_\beta$. The transition represented by T_c is purely reversible (Schwarz, 1968) and is therefore taken to be a magnetic transition and not a transition involving cation diffusion in the lattice. A transition of the latter type probably occurs around T_γ as strong thermal hysteresis depending on heating and cooling rates is observed in the change of the susceptibility (Schwarz, 1968) of Fe_9S_{10} just below T_γ. These data show that T_β represents a crystallographic change at least for compositions around Fe_7S_8, as the magnetic moments are already disordered at T_c ($T_c < T_\beta$) and the crystal symmetry appears to increase suggesting the disappearance of vacancy ordered superstructures.

Magnetic Properties of Natural Pyrrhotite

The magnetic properties of natural pyrrhotite are generally comparable to those of synthetic pyrrhotite of the same composition. However, the following modifications may apply:

1. A part of the Fe may be replaced by other elements of the transition metals group such as Ni in the natural material. Such replacements may have a strong effect on the intrinsic magnetic properties (Vaughan *et al.*, 1971).

2. The composition of natural pyrrhotite is rarely around FeS with the exception of pyrrhotite in meteorites and lunar rocks. The great majority (95% according to Arnold, 1967) of terrestrial pyrrhotite has a bulk composition between $Fe_{0.90}S$ and $Fe_{0.87}S$ and consequently falls in the two-phase field between Fe_9S_{10} and Fe_7S_8. Single-phase pyrrhotite usually has the composition Fe_7S_8 as observed for the Falconbridge Mine, Sudbury, and parts of the Meguma Formation in Nova Scotia. The determination of the composition of these phases and their relative abundance yields basic information. The strong dependence of the transition temperatures T_c, T_γ, and T_α on the composition render the thermomagnetic method of analysis attractive from the point of view of both high resolution, general applicability, and convenience as discussed in an earlier part of this paper. The measured magnetic parameters are compared to those given in the phase diagram.

The single Curie temperature of 310°C observed in Figure 6A indicates that the only pyrrhotite type present is Fe_7S_8. Its abundace in weight per cent is easily computed by taking the magnetization at 20°C acquired in H = 5350 oe:

$$J^{5350\ oe}_{20°C}\ (\text{sample}) = 11.8\ \text{emu/gram}$$

and subtracting from this the magnetization at $T \geq T_c$ extrapolated to T = 20°C:

$$J^{5350\ oe}_{310°C \rightarrow 20°C}\ (\text{sample}) = 0.18.$$

This yields the magnetization at 20°C due only to Fe_7S_8:

$$J^{5350\ oe}_{20°C}\ (Fe_7S_8) \approx 11.6.$$

The standard value for 1 gram of Fe_7S_8:

$$J^{5350\ oe}_{20°C}\ (1\ \text{gram}\ Fe_7S_8) = 15.3\ \text{emu}$$

so that the abundance of Fe_7S_8 is 11.6/15.3 = 76 weight per cent. The correction for the contribution of other minerals which becomes apparent above the Curie point of Fe_7S_8 can usually be carried out with sufficient accuracy by taking

$$J^{5350\ oe}_{310°C \rightarrow 20°C}\ (\text{sample}) \propto H/T.$$

This correction is somewhat too large because the paramagnetic contribution of the Fe_7S_8 is not considered.

Figure 6B shows two Curie points: one at 315°C (Fe_7S_8), and one at 265-270°C (Fe_9S_{10}). The abundance of Fe_7S_8 is computed first following the method described above. Then

$$J^{5350\ oe}_{20°C}\ (Fe_9S_{10}\ \text{in sample}) = J^{5350}_{20°C}\ (\text{sample}) - J^{5350}_{20°C}\ (Fe_7S_8\ \text{in sample}) - J^{5350}_{315°C \rightarrow 20°C} = 7.5\ \text{emu/gr.}$$

Since $J^{5350\ oe}_{20°C}$ (1 gram Fe_9S_{10}) = 10.2 emu, one obtains (7.5/10.2) x 100 = 74 wt % Fe_9S_{10}.

3. The natural material has only been observed in the low-temperature (below T_γ) state where Fe_9S_{10} is antiferromagnetic.

4. The low-field magnetic susceptibility of Fe_7S_8-containing samples is not an intrinsic property and therefore has not been studied for the synthetic samples. However, this property is of interest in applied geophysics.

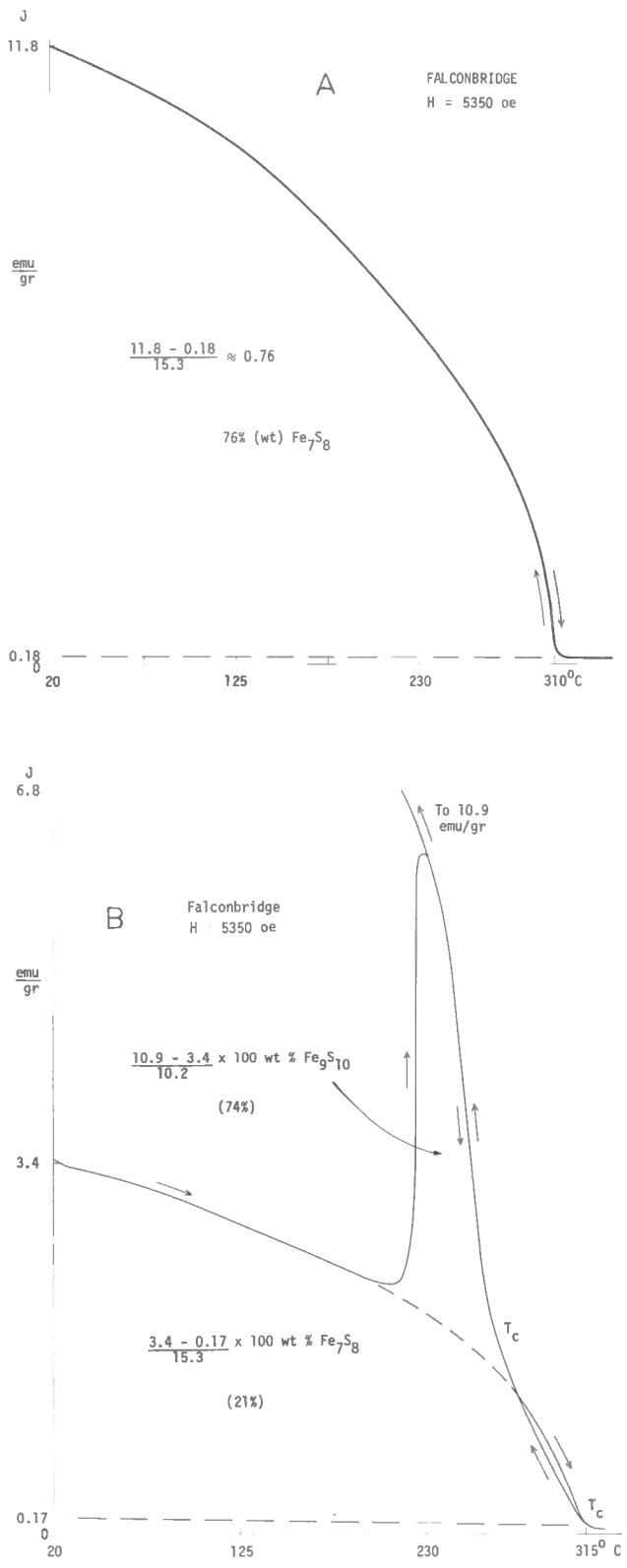

Figure 6. Analysis for pyrrhotite type and its abundance in natural specimens for a sample containing only Fe_7S_8 (A) and a sample containing both Fe_7S_8 and Fe_9S_{10} (B).

5. The strong magnetocrystalline anisotropy is an intrinsic property and can be determined for large, pure crystals of natural material and serve as a calibration standard to assess the degree of orientation in polycrystalline aggregates. The anisotropy is easily detectable by measuring the susceptibility in different directions for Fe_7S_8. Samples of high Fe_9S_{10} content may be heated to T_γ (200°C) where Fe_9S_{10} becomes ferrimagnetic and cooled rapidly before measuring the susceptibility. The basal plane orthogonal to the crystallographic C axis contains the direction of maximal susceptibility while the C axis itself represents the direction of minimal susceptibility. Fuller (1964) observed that the directions of both high susceptibility and Natural Remanent Magnetization (NRM) of slates containing pyrrhotite lie in the cleavage plane. Furthermore, he observed that the anisotropy becomes less distinct the more diluted the pyrrhotite on account of the increase in the (nearly) isotropic component of the susceptibility due to the matrix. The dependence of the anisotropy on composition and temperature has not been studied to date.

6. Another property which is of great interest in natural pyrrhotite is the direction of the Natural Remanent Magnetization (NRM). The NRM of rocks normally consists of various components of different coercivity or stability acquired at various stages in the history of the rock. One of these components usually was acquired at the time of origin of the rock either by chemical precipitation of a magnetic mineral below its Curie temperature, by cooling through the Curie temperature, or by sedimentation of magnetic grains all in the presence of an ambient magnetic field. This component must be isolated by the removal of the other components which normally have lower stability. In the case of pyrrhotite, the first two possibilities mentioned may have been operative in the production of stable remanence. To date, no information on the grain-size dependence of magnetic parameters such as coercivity is available. Natural remanence would be carried only by Fe_7S_8 and may be affected by the strong anisotropy which could cause a strong difference in direction between magnetization and the field in which it was acquired.

PART II

APPLICATIONS

The magnetic properties of pyrrhotite can be used to obtain information of prime importance in geological and geophysical studies on sulphide (ore) deposits. From a geological point of view, the spatial distribution of pyrrhotite types and their relation to wall-rocks, the relative age of a sulphide deposit with respect to wall-rocks, and the fabric in the deposit and in the wall-rocks are of considerable interest. In geophysical prospecting the spatial distribution of pyrrhotite types, the remanent magnetization, bulk susceptibility and anisotropy of susceptibility and conductivity of a sulphide deposit and those of the dominant wall-rocks are of basic interest. These applications will be discussed in the following in the light of recently obtained results and published data. The possibility of applying paleomagnetic techniques to sulphide deposits are discussed under a separate heading.

Geological Applications

1. Pyrrhotite type. The application of the thermomagnetic method of analysis to pyrrhotite-containing rocks leads to recognition of three dimensional distribution patterns of distinct $Fe_{1-x}S$ phases. This is of particular interest in sulphide deposits. For example, in the Strathcona deposit near Sudbury a roughly even distribution of Fe_7S_8 and Fe_9S_{10} was observed in the norite which abruptly changed to a single-phase Fe_7S_8 pattern (Fig. 7) in the breccia zone directly below the lower contact of the norite. With increasing depth, Fe_9S_{10} reappeared and gradually increased in average abundance to roughly 50% at 2,500 feet (Vaughan *et al.*, 1971). On the other hand, the Falconbridge deposit in the Sudbury area contains virtually only Fe_7S_8 with up to 40% of Fe_9S_{10} occurring locally at lower levels at depths of about 5,000 feet. The main ore zone is in a breccia zone stratigraphically just below the norite. Consequently, this pattern can be correlated with the pattern deduced for the Strathcona deposit as shown on Figure 7. Apparently, Little Stobie on the South Flank is also low in Fe_9S_{10} while Copper Cliff North, which is situated in a vertical offset, contains an appreciable quantity of Fe_9S_{10} (Schwarz, 1973a). This indicates pyrrhotite-type zoning as shown schematically on Figure 7.

A different distribution pattern was deduced by Takeno (1966) for the Kawayama ore body in Japan on the basis of a qualitative analysis of thermomagnetic results. He concluded that the pyrrhotite in the central part of the deposit is less Fe-deficient than in the outer parts. The interpretation of this radial change in Fe/S was the absence of a relation between the wall-rocks and the ore deposit.

2. Fabric. The fabric in a sulphide deposit is most easily determined by measuring the magnetic susceptibility of an oriented sample in various directions (Schwarz, 1973b, 1974). The results equivocally show either the preferred orientation of crystals of the ferrimagnetic Fe_7S_8 because of their very high anisotropy or layering of magnetic sulphides and non-magnetic sulphides or silicates. A distinction between both possibilities can probably be made by also measuring the anisotropy of the electrical conductivity which is expected to be high only in the case of layering. Anisotropy of magnetic susceptibility due to shape of the Fe_7S_8 crystals is not expected to have a noticeable effect. The anisotropy of antiferromagnetic Fe_9S_{10} crystals is very low but it can be greatly enhanced if desired by heating the sample to T_γ (220°C), where the Fe_9S_{10} is ferrimagnetic, and subsequent quenching to 20°C. An example of the occurrence of a consistent pattern is the sulphide ore bodies in the Sudbury area. As shown on Figure 8, the axis of the minimal susceptibiltiy is preferentially aligned northward and dipping about 45 degrees for the Strathcona deposit. This is roughly at right angles to the lower contact of the Sudbury Irruptive and suggests layering of magnetic and non-magnetic sulphides almost parallel to the contact or preferred orientation of Fe_7S_8 crystals where the C axis is preferentially aligned parallel to the minimum susceptibility direction. The other deposits show different characteristics.

The magnetic fabric of the Alexo deposit near Timmins shows that the C axis (k_{min} directions) appear

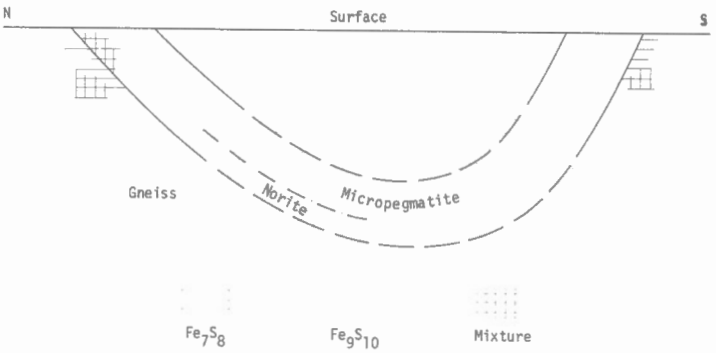

Figure 7. Evidence for pyrrhotite type zoning in the Sudbury area.

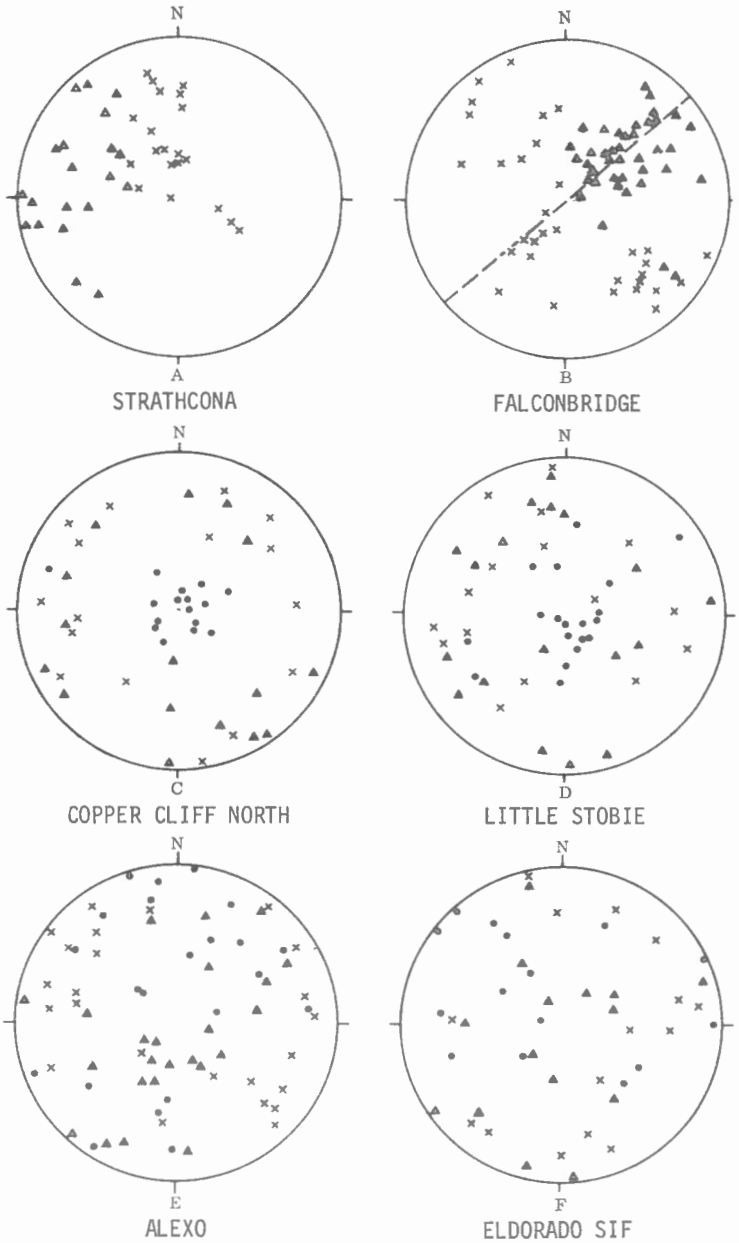

Figure 8. Spatial distribution of principal magnetic susceptibilities in some sulphide deposits in the Sudbury and Timmins areas. Dots, triangles and crosses indicate respectively maximal, intermediate and minimal susceptibility directions. Only open triangles indicate upper hemisphere projections.

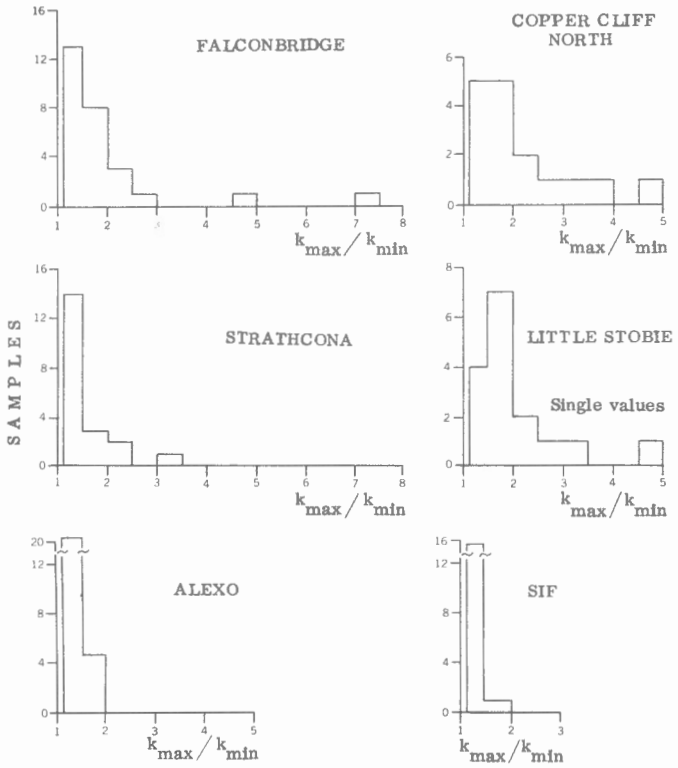

Figure 9. Histograms showing degree of anisotropy (k_{max}/k_{min}) for some sulphide deposits. Nearly isotropic magnetite (*see* Table 1) dilutes the anisotropy.

to be preferentially aligned perpendicular to the regional tectonic trend. The relatively high magnitude of the anisotropy is shown on Figure 9.

3. Thermometer. The irreversible thermomagnetic curves invariably observed for natural Fe_9S_{10} - containing samples (Fig. 6B) indicate that this material was equilibrated at low temperatures ($T<T_\gamma \approx 220^oC$). This is also indicated by the fact that Fe_7S_8 is observed in nature while it has the strong tendency to be converted to non-magnetic sulphides e.g.:

$$4\ Fe_7S_8 \rightarrow 3\ Fe_9S_{10} + FeS_2$$

between approximately 250 and 300°C (normal pressure) The use of these observations in estimating the temperature of formation is unjustifiable if only because the magnetic (ferrimagnetic) to non-magnetic (antiferromagnetic, $T<T_\gamma$) transition in Fe_9S_{10} at about $T_\gamma \approx 220^oC$ can be demonstrated in the laboratory in the course of only one day (Fig. 4D). This transition is probably due to relatively rapid diffusion of the Fe atoms between the large sulphur atoms in the lattice at ~200°C resulting in a different vacancy ordering scheme (*see* Part III).

4. Remanence. Information on relative ages of sulphide (ore bodies) and wall-rocks as well as structural information may be obtained by investigating the remanent magnetization. This is done by using paleomagnetic techniques and the amenability of rocks containing pyrrhotite for such studies is discussed in the next section of this paper.

Paleomagnetic Applications

Ferrimagnetic pyrrhotite (Fe_7S_8) usually shows appreciable natural remanent magnetization which makes it amenable to paleomagnetic studies. In many cases pyrrhotite is present as an accessory magnetic mineral which still produces an appreciable portion of the total natural remanent magnetization of a rock. It occurs over extensive areas in thick rock formations of various types such as the Meguma Group sediments and the Cape Smith basalts in Canada. However, attention must be paid to the properties of pyrrhotite of relevance in the design of paleomagnetic washing techniques. Magnetite is often observed coexisting with both finely disseminated pyrrhotite and virtually massive pyrrhotite.

So far, only a few paleomagnetic studies have been carried out on pyrrhotite-containing rocks. Hanus and Krs (1963) obtained information on the age of a sulphide deposit while Schwarz (1966) attempted to establish a relation between a sulphide deposit and a diabase dyke which was in contact with the deposit. The practical value of such studies is easily seen as this type of study would yield unique information on the relationship of the sulphide ore to various types of wall-rocks and on the tectonic evolution of the deposit. It is probable, therefore, that this type of study will be taken up in the future now that the intrinsic magnetic properties of pyrrhotite have been systematically examined.

A first requirement for meaningful paleomagnetic study is that the acquisition of remanent magnetization is virtually isotropic. Otherwise, the direction of the stable natural remanence cannot be taken to represent the direction of the ambient (paleomagnetic) field at the time and place of acquisition of this remanence. This test is easily done by allowing a demagnetized sample to acquire a remanent magnetization in a known magnetic field and probably yields a positive result only if the crystals are randomly oriented. The acquired remanence should be closely parallel to the magnetic field regardless of the orientation of the sample. The low-field susceptibility may also be used as an initial test for anisotropy.

The magnetic or thermal energy required to demagnetize a sample is a measure of the stability of the magnetization. The stability probably increases with decreasing grain size down to perhaps a few hundred Å. Consequently, finely disseminated pyrrhotite and, in particular, two-phase mixtures, are attractive for paleomagnetic work. Tests for the presence of two phases have been discussed in an earlier part of this paper.

Because in particular the low stability component of the natural remanence is subjected to change due to variations in the external field conditions, testing by using paleomagnetic washing techniques is required. In general, washing is carried out by subjecting a sample to either heating (and cooling in zero-field) or to alternating fields in the absence of a constant field. Heating can be applied preferably to monotype Fe_7S_8; the presence of Fe_9S_{10} may require very good control of the "field-free" space on account of the generation of ferrimagnetism at about 180°C and higher. The latter would cause a substantial increase in the danger of having the sample acquire a stable remanence on cooling.

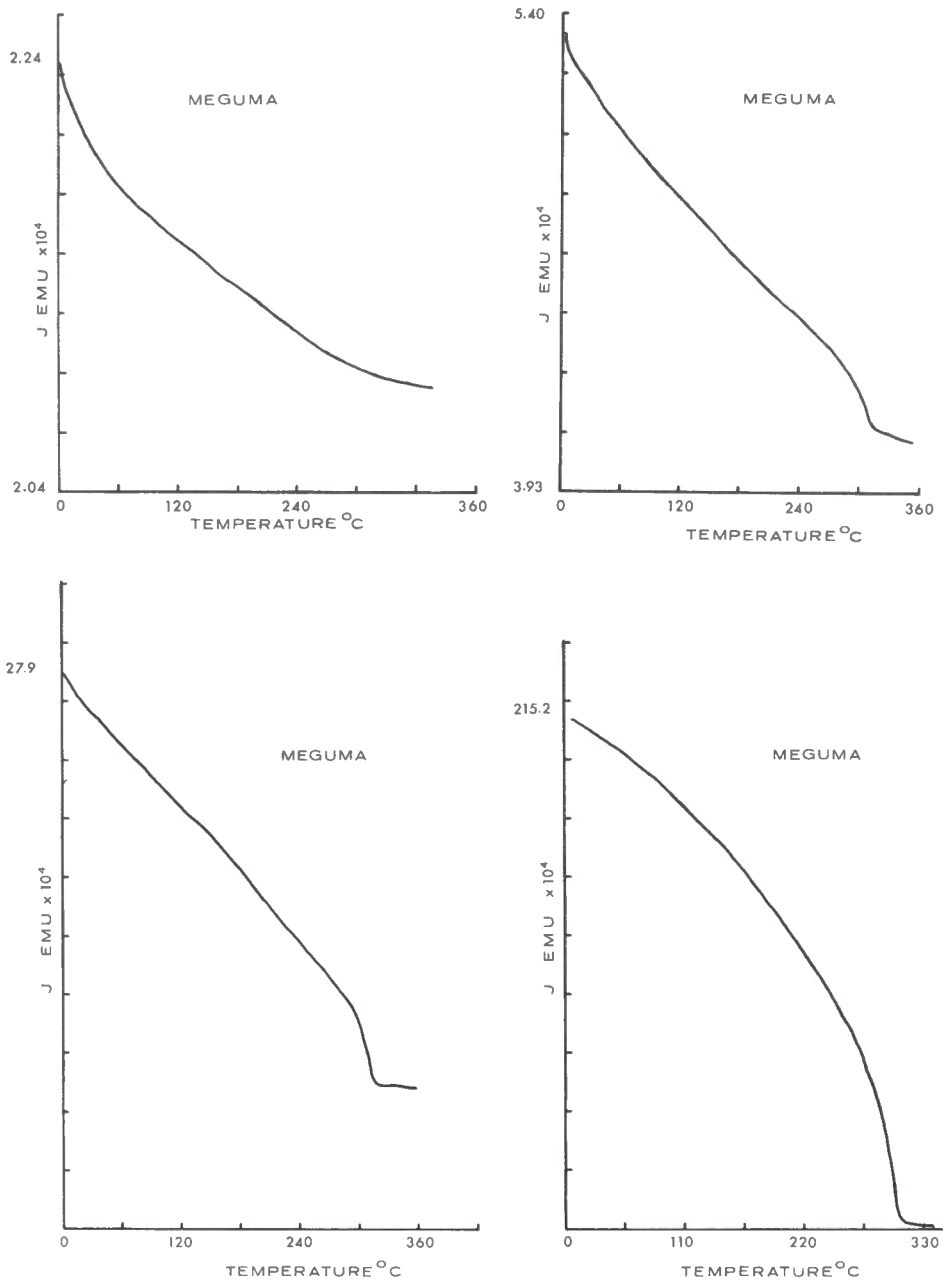

Figure 10

Thermomagnetic curves showing the gradual appearance of Fe_7S_8 for samples taken along a 100 m long line from the low background area into one of the regional aeromagnetic anomalies North of Halifax, Nova Scotia.

Heating may cause appreciable chemical change of, in particular, small samples at temperatures above 350°C (Schwarz and Harris, 1970) which is above the Curie point. This danger can be reduced by heating the sample in nitrogen or non-reactive gas. However, Fe_7S_8 may be transformed to Fe_9S_{10}+ FeS_2 above 250°C at low heating rates.

Alternating field demagnetization is commonly used as a washing technique because it has no effect on the magnetic mineralogy. However, the high electrical conductivity of pyrrhotite will have a strong screening effect, in particular in large grains, so that homogeneous demagnetization is not achieved. An estimate of the decrease in amplitude of the alternating magnetic field with depth for a cylinder of massive ferrimagnetic (Fe_7S_8) pyrrhotite can be obtained by using the skin-depth (S) at which the peak value of the applied alternating field (H_o) is reduced to $H_s = H_o/e$:

$$S = \sqrt{\frac{2\rho}{\omega \mu_o \mu}} \approx 0.3 \text{ cm.}$$

In this equation, the conductivity $\rho = 2.5 \times 10^{-5}$ Ohm/m (Keller and Frischknecht, 1966), and the permeability $\mu = 1+4 \pi k = 1.2$, while the frequency of the applied field was set at 60 cps. It is obvious that the applied demagnetizing field is very strongly attenuated with depth from the surface of a sample of massive pyrrhotite. Consequently, the method of removal of secondary components of remanent magnetization by the application of alternating magnetic fields cannot be recommended even for samples containing isolated fairly large pyrrhotite grains. On the other hand, samples containing pyrrhotite in rather diluted and finely dispersed form could be

considered for profitable treatment with this method. For comparison, the skin-depth for pure magnetite at 60 cps is roughly 1.4 cm.

Geophysical Applications

1. Exploration for massive sulphide deposits. In many sulphide (ore) deposits both magnetite (Fe_3O_4) and pyrrhotite are present as magnetic minerals. Magnetite has relatively high magnetic susceptibility and intensity of remanent magnetization unless titanium replaces iron in the lattice to a very substantial degree as in quenched basic rocks. Also, the observed remanence is in many cases stable to such a degree that its direction may differ strongly from the Earth's present field direction.

The chemical composition of magnetite is known to vary not only from rock type to rock type but also for the same rock type (i.e. basalts). The abundance of magnetite also varies from rock to rock in many cases. However, the wall-rocks of sulphide deposits usually have magnetite contents in the same range as that of the sulphide deposits. It follows that a substantial magnetic anomaly over a massive sulphide deposit is generally due to magnetic pyrrhotite (Fe_7S_8).

The weak-field magnetic susceptibility in any direction in the basal plane of a Fe_7S_8 crystal is not much lower than that of magnetite. However, it is in the paramagnetic (low) range at right angles to the basal plane. Thus, if substantial crystal orientation occurs, the magnetization induced by the Earth's field depends strongly on the directions of the maximal and minimal susceptibilities with respect to the local geomagnetic field. The signal will be relatively strong when the maximum susceptibility is parallel to the field. Massive single-phase Fe_7S_8 generally displays strong remanent magnetization parallel to the geomagnetic field due to low stability. This remanence adds to induced magnetization resulting in a positive anomaly. However, small lamellae of Fe_9S_{10} would cut down the grain size of the Fe_7S_8 and an increase in stability of the remanence may be expected. In that case the remanence may be in a direction diverging widely from the geomagnetic field resulting in a weaker signal. Thus, the direction of the total magnetization of a sulphide body may differ from the local field on account of remanence stability and magnetic anisotropy. If the total magnetization is of high intensity compared to that of the wall-rock, the shape of the sulphide body will also affect the signal, as the energy of the magnetostatic interaction of the surface charges will tend to be minimal. This is shape anisotropy and its effect is to draw the magnetization towards the long axis of the body. Thus the signal is enhanced if the geomagnetic field is closely parallel to the long axis. Predictions as to the shape must be made primarily on the basis of geological information. It follows that the characteristics of surface magnetic anomalies over sulphide deposits may show a great variation due to the complex magnetic properties of pyrrhotite.

To date, no method exists to select magnetic anomalies in prospecting for sulphide ores. However, as magnetic maps are generally available in Canada and the magnetic method of prospection is widely used, the determination of characteristics of magnetic anomalies should be worthwhile. This can only be done by determining the properties listed in Table I for samples collected from existing mines in distinct mining areas or from surface exposures in which pyrrhotite is observed, and attempting to establish correlations between pyrrhotite type or magnetic properties and for instance, type of wall-rock (Schwarz, 1973).

2. Gold deposits in clastic low-grade metamorphic rocks. Extensive regional aeromagnetic anomalies of amplitudes up to 400 γ were observed over the Meguma Formation in Nova Scotia as shown on Geological Survey maps 7030G to 7039G, 7291G. Surface sampling and thermomagnetic analyses show that the anomalies are associated with Fe_7S_8 which occurs in large lenses following the local Appalachian trend. Figure 10 shows the increasing content in Fe_7S_8 detected in samples taken while going from the low-background rocks towards the central portion of one of the anomalies. Fe_9S_{10} was detected in minor quantities in a few of the samples. It seems possible that the pyrrhotite was generated by loss of sulphur at low temperature (less than 250°C) of pyrite (FeS_2) which occurs commonly in the Meguma Formation. The anomalies could then indicate cores of anticlines or deformation zones. There seems to be a definite correlation between the presence of pyrrhotite (or positive aeromagnetic anomalies) and the occurrence of gold in the Meguma Formation (Cameron and Hood, 1974). The gold may have been mobilized and concentrated during the breakdown of auriferous pyrite and the formation of pyrrhotite in zones of metamorphism. A similar correlation has been reported for an area in the northeast part of the USSR (Izmailov, 1973).

Other Applications

Another application of the study of pyrrhotite may be in the evaluation of ore by electromagnetic induction as part of ore dressing. This would be of interest if the economic minerals can be related quantitatively or qualitatively to the occurrence of pyrrhotite in general or to specific pyrrhotite types.

The consistently higher Ni content of Fe_9S_{10} as compared to that of Fe_7S_8 and relatively high Co content of Fe_7S_8 as determined by Vaughan *et al.*, (1971) for the Strathcona Mine could be of interest in the design of methods of ore dressing. Ni and Co contents in pyrrhotite have been used by Cambel and Jarkowsky (1969) to classify pyrrhotite according to genetic type.

Table I

Feature	Strathcona	Falconbridge	Copper Cliff N	Little Stobie	Norite	Alexo	S.I.F.
$Fe_7 S_8$	∿ 45%	∿ 60%	∿ 60%	∿ 55%	∿ 0	8%	2.5%
$Fe_9 S_{10}$	∿ 15%	very low	∿ 5%	low	∿ 0	4.5%	4%
$Fe_3 O_4$	∿ 3%	∿ 1%	∿ 4%	∿ 2%	up to ∿ 7%	2%	4%
Remanent Intensity	5.10^{-2}	1.10^{-2}	7.10^{-2}	3.10^{-2}	10^{-3} to 10^{-2}	1.3×10^{-2}	3.4×10^{-2}
Remanent Direction	scattered	∿ || F	∿ || F	scattered	∿ || F	∿ || F	scattered
Remanent / Induced	2.0	1.1	3.0	1.5	up to 2.0	0.7.	0.5
Anisotropy crystal	k_{min} || F	scattered	k_{max} || F	k_{max} || F	low	k_{max}:NE-SW	scattered
Anisotropy body	k_{min} || F	$\sim k_{max}$ || F	k_{max} || F	$\sim k_{max}$ || F	low	$\sim k_{max}$ || F	$\sim k_{max}$ || F
Aeromag. Anomaly Intensity	not clear	20-40 γ	∿ 100 γ	not clear	up to ∿4000γ	not clear	not clear
Aeromag. Anomaly Sign	not clear	+	+	not clear	+	not clear	not clear
Aeromag. Anomaly Shape	not clear	Following ore body (E-W, vertical plate)	Following ore zone (NW-SE, vertical plate)	not clear	Tends to follow structure	following structure	following structure

Magnetic properties and some characteristics of aeromagnetic anomalies for sulphide deposits near Sudbury and Timmins and for the Sudbury norite.

F indicates the geomagnetic field and k_{min} and k_{max} represent respectively the minimal and maximal susceptibility directions.

The estimated average abundances are in weight percent.

PART III

FREE ENERGY AND VACANCY ORDERING

Role of the Vacancies

The magnetic properties of pyrrhotite ($Fe_{1-x}S$, $0 \leq x < 0.13$) depend on the chemical composition. This observation has been explained on the basis of a simple model of two negatively coupled, equivalent, and interpenetrating magnetic sublattices (Néel, 1953; Bertaut, 1953). For vacancy contents smaller than 8 per cent ($x<0.08$), vacancy interaction would not occur resulting in an equal distribution of the vacancies over both sublattices at least for temperatures above - 196°C. However, higher vacancy concentrations would lead to interactions and to a well-defined vacancy superstructure in Fe_7S_8 ($x = 0.125$).

The intrinsic magnetic properties vary anomalously with temperature for Fe_9S_{10}. It is tempting to hold variations in the vacancy distribution over both sublattices responsible. Antiferromagnetism occurring below ∿200°C was associated with a random distribution of the vacancies or disorder (Lotgering, 1956) while ferrimagnetism observed between ∿200°C and the Curie temperature T_c = 265°C would be the result of ordering of the vacancies on one of the sublattices. However, it is equally possible and more attractive to propose that the transition antiferromagnetism to ferrimagnetism (so-called γ transition; Haraldsen, 1941_b) is due to a change in definite ordering patterns of the vacancies rather than a vacancy disorder to order change during heating. Also, the energy levels for two different vacancy ordering patterns would be much closer than the energy difference between an ordered and disordered state.

The ordered antiferromagnetic models are based on different stacking orders of the well-established Bertaut (1953) cell for Fe_7S_8 and comply with the fact that per molecule $Fe_{1-x}S$ only discrete ratios of Fe and S occur in nature. The latter follows from the stepwise change in Curie temperature with composition (Fig. 5; *see* also Schwarz and Vaughan, 1972) and from X-ray data (Morimoto *et al.*, 1970). Vacancy-ordered antiferromagnetic models for Fe_9S_{10}, $Fe_{11}S_{12}$, and $Fe_{12}S_{13}$ are shown schematically on Figure 2, and have been discussed in some detail by Schwarz and Vaughan (1972). A new type of antiferromagnetic structure has been defined for Fe_9S_{10}, in which each crystallographic unit cell shows non-zero spontaneous magnetization directed in opposition to equal moments of the neighbouring cells in the direction of the c axis.

The new information discussed above renders a re-examination of the effects of vacancy order and magnetic order on the free energy worthwhile. Lotgering (1956) considered only vacancy ordering without magnetic order and magnetic ordering without vacancy order. A more general approach seems appropriate although the effect of within-sublattice order is difficult to evaluate. Furthermore, information on the type of bonding may be obtained. Bonding in pyrrhotite probably is partly ionic; additional components being of the covalent and d-d electron type.

Bonding

To a first approximation, the pyrrhotite system can be regarded as a binary system formed by Fe and vacancies (V). In case of purely ionic bonding, one molecule $Fe_{1-x}S$ can be represented by:

$$Fe^{2+}_{1-3x}\ Fe^{3+}_{2x}\ V_x\ S_1.$$

However, making a distinction between Fe^{2+} and Fe^{3+} in pair interaction energies probably is not crucial because the energies of V-Fe^{2+} and V-Fe^{3+} will differ only slightly. Also, Bertaut's (1953) calculation of the Madelung energy suggests that an equal distribution of Fe^{3+} over both sublattices is most favorable. Finally, Vaughan and Ridout's (1970) interpretation of Mössbauer results is that there are four different cation positions as in the Bertaut cell for Fe_7S_8 without the need of assigning specific positions to Fe^{3+}.

The number of Fe^{3+} ions required for charge balance can be strongly reduced by assuming considerable non-ionic bonding components. The high electrical conductivity, some of the Mössbauer results, and consideration of ionic radii and interionic distances in the crystal structure suggest that non-ionic bonding is an important factor (Goodenough, 1963; Ward, 1970). Then a molecule can be represented by:

$$Fe^{(2-p)+}_{1-x}\ V_x S_1^{(2-p)-}\ eh^{+}_{(2-p)x}$$

where p is proportion of covalence and $eh^{+}_{(2-p)x}$ indicates the number of electron holes which may also occur on sulphur.

Order Parameter

Following Bragg and Williams (1935), order of the vacancies over both sublattices can be described by:

$$\sigma_v = \frac{N_v^b - N_v^a}{N_v}, \quad N_v = N_v^a + N_v^b > o,$$

where N_v is the total number of vacancies per mole, and N_v^a and N_v^b represent the number of vacancies on respectively the a and b sublattices. An equal distribution of the vacancies over the sublattices is then characterized by $\sigma_v = o$ while $\sigma_v = \pm 1$ indicates that all cation vacancies are confined to one of the sublattices. Indicating the number of Fe atoms per mole by N_F and the number of Fe atoms on the a and b sublattices by N_F^a and N_F^b we can also write:

$$\sigma_v = \frac{N_F^a - N_F^b}{N_v}.$$

The total number of cation sites per mole equals $N_v + N_F$ (= N).

Magnetic (spin) order can be represented by $W_j^{a,b}(T) = M^{a,b}(T = T)/M^{a,b}(T = 0^oK)$ where $M^a(T)$ and $M^b(T)$ indicate the magnetizations of respectively the a and b sublattices. The difference of the sublattice magnetizations ($0 \leq T < T_c$): $M(0) = M^a(0) - M^b(0)$ can be obtained by extrapolating determined values for the saturation magnetization to $T = 0^oK$. This yields an estimate of the magnetic moment per molecule $Fe_{1-x}S$.

Internal Energy

The number of V-V, V-Fe and Fe-Fe pair interactions per mole and their energies are denoted respectively by N_{vv}, N_{vF}, N_{FF}, and e_{vv}, e_{vF}, e_{FF}. The internal energy is the sum of the energy involved in bonding in the crystal (E_b) and the energy involved in magnetic interactions. The expression for E_b is a summation over its ith neighbour pairs:

$$E_b = \sum_i \left[N_{vv}(i)\, e_{vv}(i) + N_{vF}(i)\, e_{vF}(i) + N_{FF}(i)\, e_{FF}(i) \right]$$

Now, $2N_{vv}(i) = Z(i)\, N_v - N_{vF}(i)$

and $2N_{FF}(i) = Z(i)\, N_F - N_{vF}(i)$,

where Z(i) represents the number of ith nearest neighbours of any vacant or occupied Fe site. Substitution yields:

$$E_b = \sum_i \frac{Z(i)}{2} \left(N_v e_{vv}(i) + N_F e_{FF}(i) \right) + \sum_i N_{vF}(i)\, \mu_{vF}(i),$$

$$\text{where } \mu_{vF}(i) = e_{vF}(i) - \tfrac{1}{2} e_{vv}(i) - \tfrac{1}{2} e_{FF}(i)$$

The first term in the expression for E_b depends on the chemical composition but not on the order parameter σ_v. However, $N_{vF}(i)$ in the second term depends on σ_v. For instance a random distribution yields:

$$N_{vF}(i) = \frac{2}{N} \left[Z^s(i) \left(N_v^a N_F^a + N_v^b N_F^b \right) + Z^o(i) \left(N_v^a N_F^b + N_v^b N_F^a \right) \right] =$$

$$= \frac{Z^s(i)}{N} \left(N_v N_F - \sigma_v^2 N_v^2 \right) + \frac{Z^o(i)}{N} \left(N_v N_F + \sigma_v^2 N_v^2 \right),$$

where $Z(i) = Z^s(i) + Z^o(i)$, indicating respectively the number of the neighbours in the same (s) and in the other (o) sublattice. However, the sublattices being equivalent, this expression is expected to be meaningful only in the case $\sigma_v = 0$ which corresponds to Lotgering's (1956) disordered antiferromagnetic model. Thus, for Lotgering's model,

$$N_{vF}(i) = Z(i)\, N_v N_F / N.$$

The ordered antiferromagnetic model proposed by Schwarz and Vaughan (1972) is characterized by $\sigma_v = 0$ and within sublattice order without the constraint of virtually constant vacancy - vacancy separation as in the Bertaut model for Fe_7S_8 but with a minimum separation of $\sim 6.9\text{Å}$. In that case:

$$N_{vv}(i) = 0, \text{ and } N_{vF}(i) = Z(i)\ N_v,$$

if i corresponds to pair separations less than 6.9Å. This is always larger than $N_{vF}(i)$ for Lotgering's model as only $N_F/N<1$ is considered here. As expected, this yields a higher E_b value for the ordered model.

The magnetic interaction energy can be represented by a summation of the spin-pair interaction terms of Heisenberg:

$$E_m = \sum_i -2\ J_i\ N_{FF}(i)\ \bar{S}_k.\bar{S}_1,$$

where J_i is the exchange integral for ith neighbour pairs. The summation over all spins in the sublattices yields the sublattice magnetizations:

$$M_a = N_F{}^a A\ W_j{}^a(T) = \tfrac{1}{2}\ (N_F + N_v\ \sigma_v)\ A\ W_j{}^a\ (T)$$

and

$$M_b = N_F{}^b\ A\ W_j^b\ (T) = \tfrac{1}{2}\ (N_F - N_v\ \sigma_v)\ A\ W_j{}^b\ (T),$$

where W_j^a (T) and W_j^b (T) are the magnetic interaction terms of cations with quantum number j defined earlier and A indicates the average moment per Fe ion.

In the above expression for E_m, $N_{FF}(i)$ depends on the vacancy arrangement. Taking a random arrangement as in Lotgering's model:

$$N_{FF}(i) = \tfrac{1}{2}\ Z(i)\ N_F\ (1-N_v/N) = \frac{1}{2N}\ Z(i)\ N_F{}^2.$$

substitution yields:

$$E_m = -\frac{1}{N} \sum_i\ J_i \left[Z^s(i)\ (M_a{}^2 + M_b{}^2) + 2\ Z^o\ (i)\ M_a\ M_b\right]$$

Again limiting the pair separation for interaction gives for the ordered model:

$$N_{FF}(i) = \tfrac{1}{2}\ Z(i)\ (N_F - N_v) = \frac{N_F - N_v}{2\ N_F}\ Z(i)\ N_F{}^2.$$

Substitution yields:

$$E_m = -\frac{N_F - N_v}{N_F{}^2} \Sigma_i\ J_i \left[Z^s(i)\ (M_a{}^2 + M_b{}^2) + 2Z^o(i)\ M_a\ M_b\right].$$

Entropy

The entropy can also be expressed as the sum of two parts. One is due to the configuration of the cations (S_c) and the other is due to the configuration of the spin moments (S_m).

Assuming a random distribution of the cations within the sublattices yields:

$$S_c = k \log \left[\frac{(N/2)!\ (N/2)!}{(N_F{}^a)!\ (N_F{}^b)!}\right]$$

Using Stirling's approximation one obtains:

$$S_c = k\left[N \log (N/2) - N_v - \frac{(N_v\sigma_v + N_F)}{2} \log \frac{(N_F + N_v\sigma_v)}{2} - \frac{N_F - N_v\sigma_v}{2} \log \frac{N_F - N_v\sigma_v}{2}\right].$$

The contribution to the entropy due to magnetic order can also be represented on the basis of the number of different ways to distribute the spins. Following essentially Lotgering (1956) but allowing for $\sigma_v = o$ gives:

$$S_m = -k\, N_F \left[\frac{3j}{j+1} \frac{T_c}{T} \left(W_j^a(T) + W_j^b(T)\right)^2 - \log \sum_{m_j=-j}^{+j} \exp\left(\frac{3}{j+1} \frac{T_c}{T} \left(W_j^a(T) + W_j^b(T)\right) m_j\right)\right]$$

The summation is taken over the $(2j + 1)$ magnetic sublevels. The disordered state, expected to occur above the Curie temperature T_c, is characterized by $W_j^a(T) = W_j^b(T) = 0$. This yields:
$S_m = k\, N_F \log (2j + 1)$, which is to be expected from the consideration that there are $(2j + 1)^{N_F}$ ways to distribute the spins over $(2j + 1)$ sublevels per site.

Free Energy

The free energy, F, can be evaluated on the basis of the expressions found for the internal energy and the entropy:

$$F \equiv E_b + E_m - T\,(S_c + S_m).$$

Consideration of within - sublattice order makes the calculations enormously elaborate. Therefore, only random distributions are considered here for $0 \le \sigma_v \le 1$. This gives the best useful approximation.

Under equilibrium conditions, the free energy will be minimal. Consequently, the partial derivations $\delta F/\delta\sigma_v$, $\delta F/\delta W_j^a(T)$, and $\delta F/\delta W_j^b(T)$ must be set to zero, and the nine second partial derivations should be positive. The first derivatives are:

$$\frac{\delta F}{\delta \sigma_v} = \sum_i \left[\frac{2\sigma_v N_v^2}{N}(Z^o(i) - Z^s(i))\,\mu_{vF}(i)\,\frac{N_v A^2 J_i}{2N}\left\{Z^s(i)\,(N_F + N_v\sigma_v)\,(W_j^a(T))^2 + \right.\right.$$

$$\left.\left. + (N_v\sigma_v - N_F)\,(W_j^b(T))^2 - 2Z^o(i) N_v\sigma_v W_j^a(T)\, W_j^b(T)\right\}\right] - \frac{kTN_v}{2} \log\left(\frac{N_F - N_v\sigma_v}{N_F - N_v\sigma_v}\right)$$

$$\frac{\delta F}{\delta W_j^a(T)} = \sum_i \left[\frac{-A^2 J_i}{2N}\left\{Z^s(i)(N_F + N_v\sigma_v)^2 W_j^a(T) + Z^o(i)(N_F^2 - N_v^2\sigma_v^2) W_j^b(T)\right\}\right] -$$

$$-kN_F\left(2r - \frac{\sum_{m_j=-j}^{+j} -j \frac{3T_c}{(j+1)\,T}\, m_j \exp(rm_j)}{\sum_{-j}^{+j} \exp(rm_j)}\right)$$

$$\frac{\delta F}{\delta W_j^b(T)} = \sum_i \left[\frac{-A^2 J_i}{2N}\left\{Z^s(i)(N_F - N_v\sigma_v)^2 W_j^b(T) + Z^o(i)\,(N_F^2 - N_v^2\sigma_v)^2\, W_j^a(T)\right\}\right] -$$

$$-kN_F\left(2r - \frac{\sum_{-j}^{+j} \frac{3T_c}{(j+1)\,T}\, m_j \exp(rm_j)}{\sum_{-j}^{+j} \exp(rm_j)}\right)$$

where $r = \dfrac{3T_c}{(j+1)\,T}\,(W_j^a(T) + W_j^b(T))$.

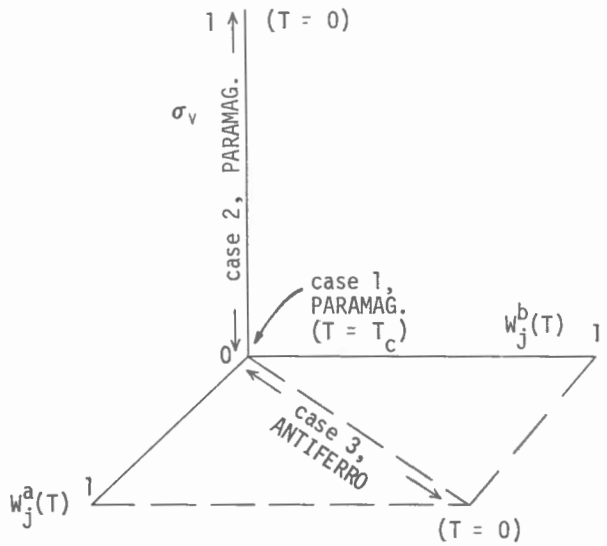

Figure 11. General magnetic phase diagram for a fixed composition representing the general solution and magnetic states described in the text.

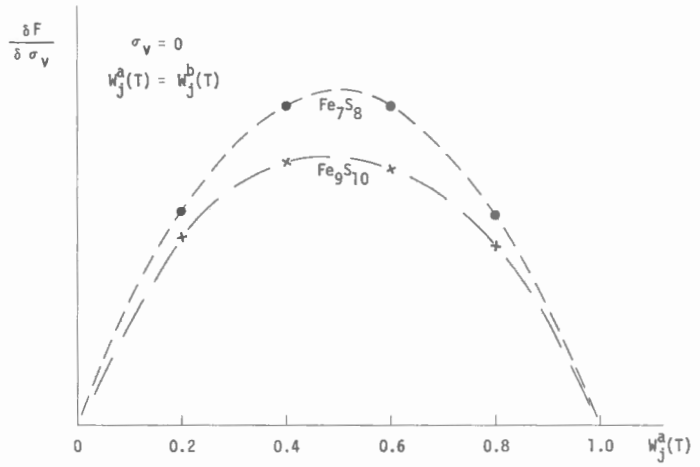

Figure 12. Dependence of the derivative of the free energy (F) with respect to the vacancy order parameter σ_v on the sublattice magnetic order parameters $W_j^a(T)$ and $W_j^b(T)$ for $\sigma_v = 0$ and for Fe_7S_8 and Fe_9S_{10}.

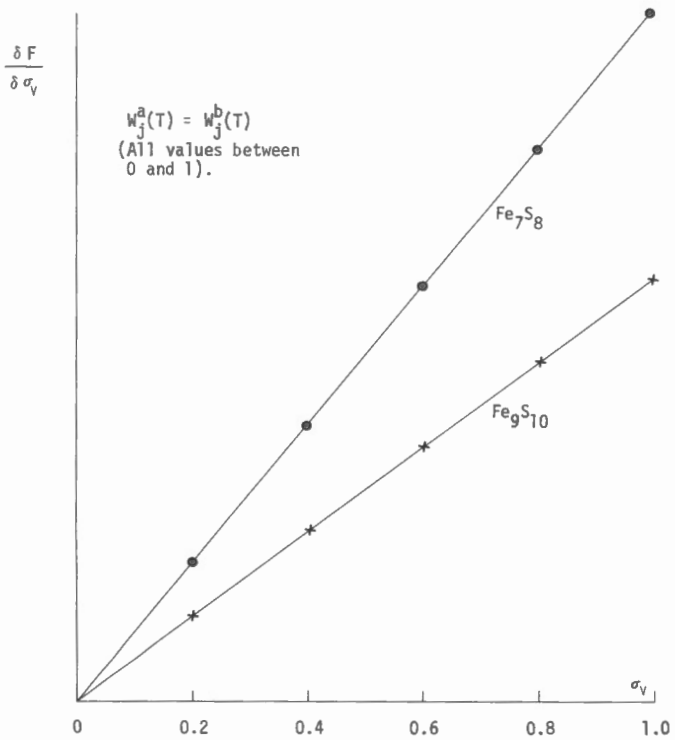

Figure 13. Linear dependence of $\delta F/\delta\sigma_v$ on σ_v for all $W_j^a(T) = W_j^b(T)$. In present case of two equivalent sublattices $W_j^a(T) \neq W_j^b(T)$ for $\sigma_v \neq 0$.

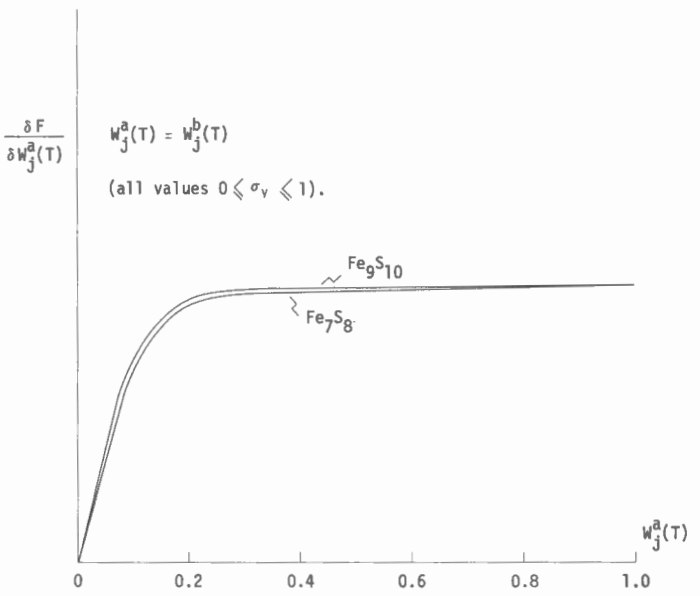

Figure 14. Dependence of $\delta F/\delta W_j^a(T)$ on $W_j^a(T)$ for Fe_7S_8 and Fe_9S_{10}.

The following general cases can be distinguished by setting these equations to zero:

1. $\sigma_v = 0$, $W_j^a(T) = W_j^b(T) = 0$.

This is the general solution and it represents the disordered paramagnetic case which occurs at $T > T_c$.

2. $\sigma_v \neq 0$, $W_j^a(T) = W_j^b(T) = 0$.

This state is also paramagnetic as $M(T) = M_a(T) - M_b(T) = 0$ $(T > T_c)$.

3. $\sigma_v = 0$, $W_j^a(T) \neq 0$, $W_j^b(T) \neq 0$

In $Fe_{1-x}S$, the magnetic sublattices are equivalent if there is no configurational long range order (disordered vacancies). Consequently, $W_j^a(T) = W_j^b(T)$ and thus $M_a(T) = -M_b(T)$. This corresponds to the disordered antiferromagnetic state as proposed by Lotgering (1956).

4. $\sigma_v \neq 0$, $W_j^a(T) \neq 0$, $W_j^b(T) \neq 0$.

This is the general magnetic case for which the equation system formed by $\delta F/\delta\sigma_v$, $\delta F/ W_j^a(T)$, and $\delta F/\delta W_j^b(T)$ must be solved. Each of these equations represents a surface in $(\sigma_v, W_j^a(T), W_j^b(T))$ space and stable conditions will be given by the intersection of the surfaces.

For each composition, the magnetic states 1 to 4 and their relationships can be displayed as in Figure 11. A numerical evaluation of the first derivatives with a computer has been attempted to see if zero values occur other than those discussed under the general solution 1, 2, and 3.

Numerical Evaluation of Free Energy

The most serious problem in evaluating the system formed by the three first derivatives is to appraise realistically the pair interaction energies combined in the term $\mu_{vF}(i)$ in the expression for the internal energy. Mathematically, the least elaborate model is to assume ionic bonding, point charges, without electron screening. In the case of pyrrhotite, this assumption yields a value for the electrostatic part of the internal energy which is more than 10^6 times the second factor, the entropy. The effect of magnetic coupling on the energy is negligible. Some results of a numerical evaluation with a computer are shown on Figure 12, which shows $\delta F/\delta\sigma_v$ for $\sigma_v = 0$ and therefore $W_j^a(T) = W_j^b(T)$ as the sublattices are equivalent. For $W_j^a(T) = W_j^b(T) = 1$, $(T = 0^oK)$, $\delta F/\delta\sigma_v = 0$. This corresponds to a maximum value of F. For $W_j^a(T) = W_j^b(T) = 0$, $(T \geq T_c)$, $\delta F/\delta\sigma_v$ also equals zero corresponding to a maximum in F. This conforms to expectations. For $\sigma_v \neq 0$, $\delta F/\delta\sigma_v$ assumes very large negative values under the assumption of ionic bonding. These are probably unrealistic.

Figure 13 shows that $\delta F/\delta\sigma_v$ depends linearly on σ_v for any value $0 \leq W_j^a(T) \leq 1$. As expected, the dependence is strongest for the more Fe deficient composition. Only $\sigma_v = 0$ results in $\delta F/\delta\sigma_v = 0$. Figure 14 shows the dependence of $\delta F/\delta W_j^a(T)$ on $W_j^a(T)$ for all values of σ_v for both Fe_9S_{10} and Fe_7S_8. The relatively Fe rich composition Fe_9S_{10} shows a slightly higher dependency. The value for $\delta F/\delta W_j^a(T)$ is always positive but extremely small for $W_j^a(T) = 0$. The expression for $\delta F/\delta W_j^a(T)$ shows that the terms containing the pair energies $(\mu_{vF}(i))$ play no role in the evaluation of $\delta F/\delta W_j^a(T)$.

Saturation Magnetization

The spontaneous magnetization (M(T)) is the difference between the sublattice magnetizations:

$$M(T) = |M_a(T) - M_b(T)| = |N_v \sigma_v A(W_j^a(T) - W_j^b(T))| \mu_B.$$

The average magnetic moment per Fe atom (A) can be obtained from experimental data on the thermal dependence of the moment M(T). Extrapolation of results obtained by Besnus and Meyer (1964) and Schwarz (1968) yields an estimated maximum value of 25 cgs emu per gram Fe_7S_8 at 0^oK. At this temperature, $|\sigma_v| = 1$ which yields $A \approx 3\mu_B$. This value for A is well below the spin - only values for the moments of $Fe^{2+}(4\mu_B)$ and $Fe^{3+}(5\mu_B)$.

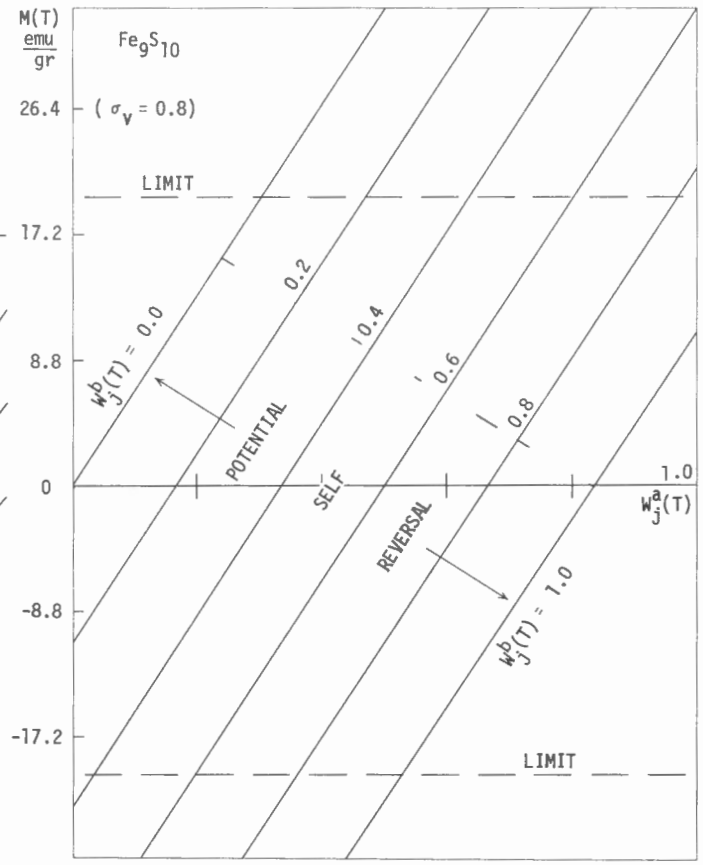

Figure 16. (above)

Dependence of the magnetization M(T) on the order parameters $W_j^a(T)$ and $W_j^b(T)$ for fixed σ_v(=0.8) for Fe_9S_{10}. The limits for M(T) are set on the basis of extrapolation of experimental results. The combination of $W_j^a(T)$ and $W_j^b(T)$ yielding M(T) values over these limits are unlikely to occur. A potential self-reversal of magnetization field is indicated but is unlikely to occur because in the case of pyrrhotite the magnetic structure is described as two equivalent sublattices.

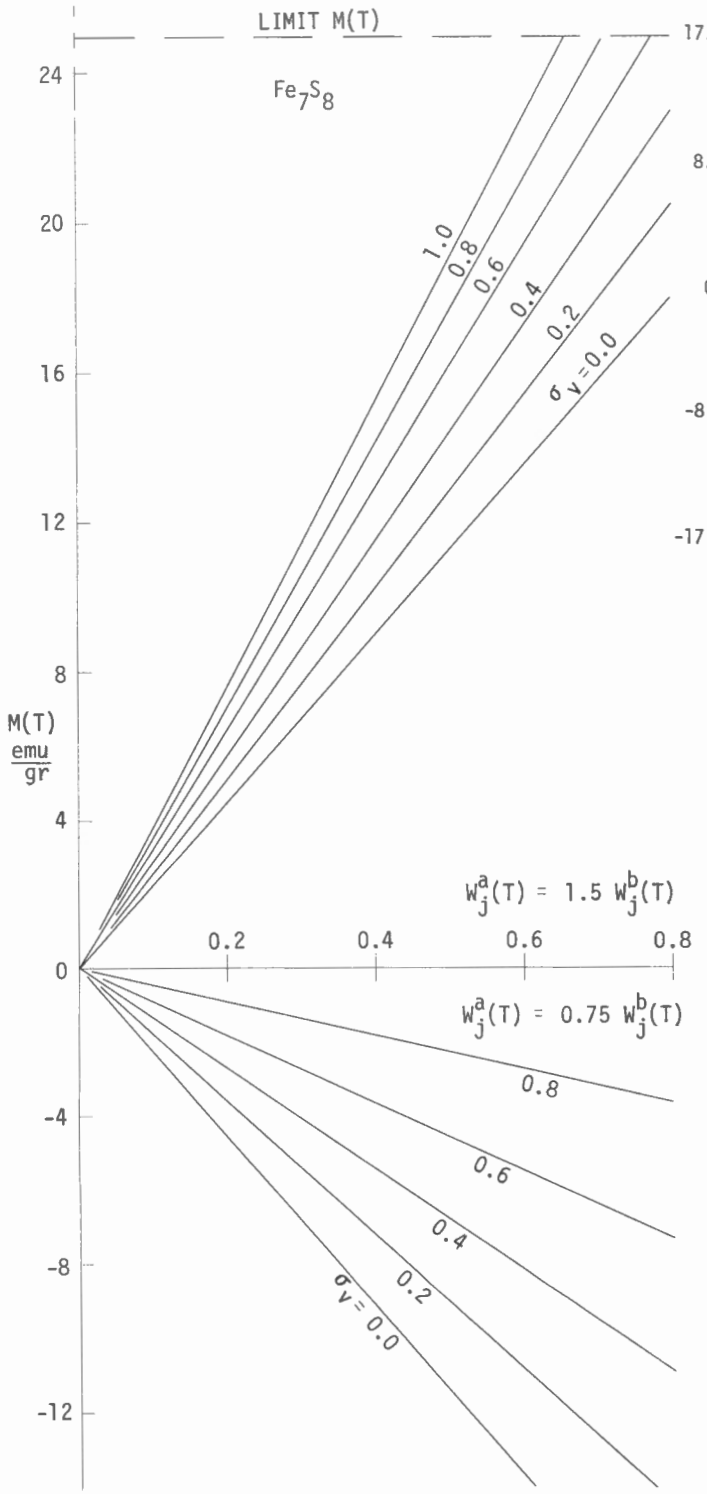

Figure 15. (left)

Dependence of the magnetization M(T) on σ_v for fixed ratios $W_j^a(T)/W_j^b(T)$. In general, σ_v = 1.0 at 0°K and decreases rapidly to zero at the vacancy disordering temperature which for pyrrhotite is higher than the magnetic disordering temperature or Curie point. It is clear that if $W_j^a(T)/W_j^b(T)$ varies with temperature the magnetization could vary in a complex manner. This does not occur for Fe_7S_8.

Representing a molecule of Fe_7S_8 by $Fe^{2+}_{5/8}\ Fe^{3+}_{2/8}\ F_{1/8}S^{2-}_{1}$, assuming ionic bonding, the average spin moment per Fe ion comes to 4.2 μ_B. Considering also orbital moments is if anything likely to increase this value according to Hund's rules although these moments are generally quenched by the inhomogeneous electric field set up by the neighbouring ions. Consequently, the low value for the average moment is due to other causes one of which may well be collective d electrons on iron resulting in a lower magnetic moment. This is strong evidence against purely ionic bonding.

The moment M(T) has been evaluated for various combinations of the order parameters σ_v, $W^a_j(T)$, and $W^b_j(T)$ and for several compositions with the help of a computer. The results for Fe_7S_8 are shown on Figures 15 and 16. Figure 15 shows the linear dependency of M(T) on σ_v for the following cases:

(a) $W^a_j(T) = W^b_j(T)$, which may occur for all σ_v values

(b) $W^a_j(T) = 1.5\ W^b_j(T)$, which could occur if $\sigma_v \neq 0$.

(c) $W^a_j(T) = 0.75\ W^b_j(T)$ which could occur if $\sigma_v \neq 0$.

The lack of comparison between the curves shown on Figure 15 and those presented on Figures 12 and 14 also indicates that the magnetization has no noticeable effect on the free energy.

Figure 16 shows M(T) as a function of the magnetic order parameters keeping σ_v fixed (= 0.8). It is obvious that changes in the relative magnitudes of the order parameters can result in marked changes of the saturation moment. Self-reversal of spontaneous magnetization is possible but not likely to occur in a system with two equivalent magnetic sublattices and σ_v should not change sign. Also, the maximum value of M(T) as determined from extrapolated experimental results puts constraints on the possible combinations of the order parameters.

References

Anderson, P.W.,
1950: Antiferromagnetism. Theory of superexchange interaction; Phys. Rev., v. 79, no. 2, p. 350-356.

Andresen, A.F. and Torbo,
1967: Phase transitions in Fe_xS (x = 0.90 - 1.00) studied by neutron diffraction; Acta Chem. Scand., v. 21, p. 2841-2848.

Arnold, G.,
1967: Range in composition and structure of 82 natural terrestrial pyrrhotites; Can. Mineral, v. 9, no. 1, p. 31-50.

Bertaut, E.F.,
1953: Contribution à l'étude des structures lacunaires, la pyrrhotine; Acta Cristallog, v. 6, p. 557-561.

Besnus, M.J. and Meyer, A.J.P.,
1964: Nouvelles données experimentals sur le magnétisme de la pyrrhotine naturelle; Inst. Phys. & Phys. Soc., Proc. Int. Conf. Magnetism, Nottingham, p. 507-511.

Bragg, W.L. and Williams, E.J.,
1935: The effect of thermal agitation on atomic arrangement in Alloys II; Proc. Roy. Soc., London, A, v. CLI, p. 540-567.

Cambel, B. and Jarkovsky, J.,
1969: Geochemistry of pyrrhotite of various genetic types; Univerzita Komenskeho; Bratislava, 333 p.

Cameron, G.W. and Hood, P.J.,
1974: Magnetic anomalies of the Meguma Group of Nova Scotia and their relationship to gold mineralization; Geol. Surv. Can., in preparation

Desborough, G.A. and Carpenter, R.M.,
1965: Phase relations of pyrrhotite; Econ. Geol., v. 60, p. 1431-1450.

Fuller, M.D.,
1964: On the magnetic fabrics of certain rocks. J. Geol., 72, 3, 368-376.

Goodenough, J.B.,
1963: Magnetism and the chemical bond; Interscience, John Wiley Sons, New York, 393 pp.

Graham, A.R.,
1969: Quantitative determination of hexagonal and monoclinic pyrrhotites by X-ray diffraction; Can. Mineral., v. 10, p. 4-24.

Graterol, M. and Naldret, A.J.,
1971: Mineralogy of the Marbridge No. 3 and No. 4 nickel-iron sulphide deposits; Econ. Geol; v. 66, p. 886-900.

Hanus, V. and Krs, M.,
1963: Uber die Anwendung des Palaomagnetismus zur Altersbestimmung hydrothermaler Erzlagerstatten, Neues Jhrb. Mineral., v. 100, no. 1, p. 87-100.

Haraldsen, H,
1941a: Uber die Eisen (II)- Sulphidmischkristalle. Zeits. anorg. allgem. Chem. v. 246, p. 169-194.

1941b: Uber die Hochtemperaturumwandlungen der Eisen-Sulphid mischkristalle; Zeits. anorg. allgem. Chem; v. 246, p. 195-226.

Hayase, K., Otsuka, R., and Mariko, T.,
1963: On the magnetic properties of natural pyrrhotite; Min. J. Japan, v. 1, p. 41-56.

Hirone, T., Maeda, S., and Tsuya, N.,
1954: On the λ-shaped ferrimagnetism of Fe $S_{1.10}$; J. Phys. Soc. Japan, v. 9, p. 736-739.

Izmailov, L.I.,
1973: Linear magnetic anomalies of the upper stream of the Kolyma River (NE of USSR); Abstract. IAGA Bull., v. 34, p. 285.

Keller, G.V. and Frischknecht, F.C.,
1966: Electrical methods in geophysical prospecting; Pergamon Press, Oxford, 517 p.

Lotgering, F.K.,
1956: Ferrimagnetism of sulphides and oxydes; Philips Res. Reports II, p. 190-217.

Morimoto, N., Nakazawa, H., Nishiguchi, K. and Tokonami, M.,
1970: Pyrrhotites: Stoichiometric compounds with composition Fe_{n-1} S_n ($n \geq 8$); Science, v. 168, p. 964-966.

Néel, L.,
1948: Propriétes magnétiques des ferrites; ferrimagnétisme et antiferromagnétisme; Ann. de Phys., v. 12, no. 3, p. 10-198.

1953: Some new results on antiferromagnetism and ferrimagnetism; Rev. Mod. Phys., v. 25, p. 58-63.

Schwarz, E.J.,
1966: Magnetization of Precambrian sulphide deposits and wall rocks from the Noranda district, Canada; Geophysics, v. XXXI, no. 4, p. 797-802.

1968: Magnetic phases in natural pyrrhotite $Fe_{0.91}S$; J. Geomag. Geoelec., v. 20, p. 67-74.

1973a: Magnetic characteristics of massive sulphide ore bodies near Sudbury, Canada; Can. J. Earth Sci., v. 10, no. 12, p. 1735-1743.

1973b: Fabric from magnetic anisotropy: Sulphide deposits near Sudbury, Ontario; *in* Report of Activities November 1972 to March 1973, Geol. Surv. Can., Paper 73-1, pt. B., p. 211.

1974: Magnetic fabric in massive sulphide deposits; Can. J. Earth. Sci., v. 11, 12, p. 1669-1677.

Schwarz, E.J. and Harris, D.C.,
1970: Phases in natural pyrrhotite and the effect of heating on their magnetic properties and composition; J. Geomag. Geoelec., v. 22, no. 4, p. 463-470.

Schwarz, E.J. and Vaughan, D.J.,
1972: Magnetic phase relations of pyrrhotite; J. Geomag. Geoelec., v. 24, no. 4, p. 441-458.

Sugaki, A. and Shima, H.,
1966: Studies on the pyrrhotite group minerals; J. Japan Assoc. Min. Pet. Econ. Geol., 55, 242-253.

Takeno, S.,
1966: Magnetometric and röntgenometric studies of pyrrhotite from the Kawayama Mine, Japan; J. Sci. Hiroshima Univ., Ser. C., v. 5, p. 113-156.

Taylor, L.A.,
1970: Low temperature phase relations in the Fe-S system; Carnegie Inst., Washington, Yb, v. 68, p. 259-270.

Vaughan, D.J. and Ridout, M.S.,
1970: Mössbauer study of pyrrhotite (Fe_7S_8); Solid State comm., v. 8, p. 2165-2167.

Vaughan, D.J., Schwarz, E.J. and Owens, D.R.,
1971: Pyrrhotites from the Strathcona Mine, Sudbury, Canada: A thermomagnetic and mineralogical study; Econ. Geol., v. 66, p. 1131-1144.

Ward, J.C.,
1970: The structure and properties of some iron sulphides. Rev. Pure and Appl. Chem., v. 20, p. 175-206.

Wollan, E.O.,
1960: Magnetic coupling in crystalline compounds. A phenomenological theory of magnetism in 3d metals; Phys. Rev., v. 117, no. 2, p. 387-401.